UC-403
LBL-27914
NDC-6

NAGRA-DOE
COOPERATIVE
PROJECT REPORT

Analysis of Well Test Data from Selected Intervals in Leuggern Deep Borehole — Verification and Application of PTST Method

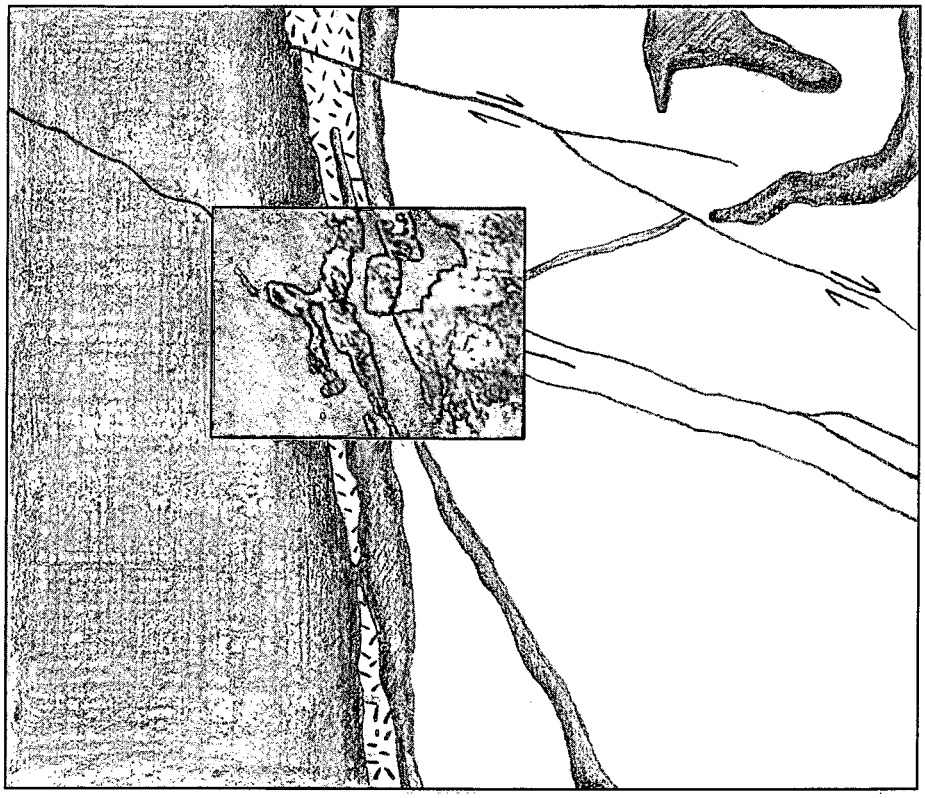

Kenzi Karasaki

July 1990

For Reference

Not to be taken from this room

Swiss National Cooperative for
the Storage of Nuclear Waste
NAGRA
CH-5401 Baden, Switzerland

Earth Sciences Division
Lawrence Berkeley Laboratory
University of California
Berkeley, California 94720, USA

Prepared for the U.S. Department of Energy under Contract DE-AC03-76SF00098

LBL-27914
Copy 1
Bldg. 50 Library.

DISCLAIMER

This document was prepared as an account of work sponsored by the United States Government. While this document is believed to contain correct information, neither the United States Government nor any agency thereof, nor the Regents of the University of California, nor any of their employees, makes any warranty, express or implied, or assumes any legal responsibility for the accuracy, completeness, or usefulness of any information, apparatus, product, or process disclosed, or represents that its use would not infringe privately owned rights. Reference herein to any specific commercial product, process, or service by its trade name, trademark, manufacturer, or otherwise, does not necessarily constitute or imply its endorsement, recommendation, or favoring by the United States Government or any agency thereof, or the Regents of the University of California. The views and opinions of authors expressed herein do not necessarily state or reflect those of the United States Government or any agency thereof or the Regents of the University of California.

LBL-27914
NDC-6

Analysis of Well Test Data from Selected Intervals in Leuggern Deep Borehole— Verification and Application of PTST Method

Kenzi Karasaki

Earth Sciences Division
Lawrence Berkeley Laboratory
University of California
Berkeley, California 94720

July 1990

This work was supported by the Manager, Chicago Operations, Repository Technology Program, Repository Technology and Transportation Division, of the U.S. Department of Energy under Contract No. DE-AC03-76SF00098 and by the Swiss National Cooperative for the Storage of Nuclear Waste (NAGRA).

Preface

This report is one of a series documenting the results of the Nagra-DOE Cooperative (NDC-I) research program in which the cooperating scientists explore the geological, geophysical, hydrological, geochemical, and structural effects anticipated from the use of a rock mass as a geologic repository for nuclear waste. This program was sponsored by the U. S. Department of Energy (DOE) through the Lawrence Berkeley Laboratory (LBL) and the Swiss Nationale Genossenschaft für die Lagerung radioaktiver Abfälla (Nagra) and concluded in September 1989. The principal investigators are Jane C. S. Long, Ernest L. Majer, Karsten Pruess, Kenzi Karasaki, Chalon Carnahan and Chin-Fu Tsang for LBL and Piet Zuidema, Peter Blümling, Peter Hufschmied and Stratis Vomvoris for Nagra. Other participants will appear as authors of the individual reports. Technical reports in this series are listed below.

1. Determination of Fracture Inflow Parameters with a Borehole Fluid Conductivity Logging Method by Chin-Fu Tsang, Peter Hufschmied, and Frank V. Hale (NDC-1, LBL-24752).
2. A Code to Compute Borehole Fluid Conductivity Profiles with Multiple Feed Points by Frank V. Hale and Chin-Fu Tsang (NDC-2, LBL-24928; also NTB 88-21).
3. Numerical Simulation of Alteration of Sodium Bentonite by Diffusion of Ionic Groundwater Components by Janet S. Jacobsen and Chalon L. Carnahan (NDC-3, LBL-24494).
4. P-Wave Imaging of the FRI and BK Zones at the Grimsel Rock Laboratory by Ernest L. Majer, John E. Peterson Jr., Peter Blümling, and Gerd Sattel (NDC-4, LBL-28807).
5. Numerical Modeling of Gas Migration at a Proposed Repository for Low and Intermediate Level Nuclear Wastes at Oberbauenstock, Switzerland by Karsten Pruess (NDC-5, LBL-25413).
6. Analysis of Well Test Data from Selected Intervals in Leuggern Deep Borehole — Verification and Application of PTST Method by Kenzi Karasaki (NDC-6, LBL-27914).
7. Shear Wave Experiments at the U. S. Site at the Grimsel Laboratory by Ernest L. Majer, John E. Peterson Jr., Peter Blümling, and Gerd Sattel (NDC-7 LBL-28808).
8. The Application of Moment Methods to the Analysis of Fluid Electrical Conductivity Logs in Boreholes by Simon Loew, Chin-Fu Tsang, Frank V. Hale, and Peter Hufschmied (NDC-8, LBL-28809).
9. Numerical Simulation of Cesium and Strontium Migration through Sodium Bentonite Altered by Cation Exchange with Groundwater Components by Janet S. Jacobsen and Chalon L. Carnahan (NDC-9, LBL-26395).
10. Theory and Calculation of Water Distribution in Bentonite in a Thermal Field by Chalon L. Carnahan (NDC-10, LBL-26058).
11. Prematurely Terminated Slug Tests by Kenzi Karasaki (NDC-11, LBL-27528).
12. Hydrologic Characterization of Fractured Rocks — An Interdisciplinary Methodology by Jane C. S. Long, Ernest L. Majer, Stephen J. Martel, Kenzi Karasaki, John E. Peterson Jr., Amy Davey, and Kevin Hestir, (NDC-12, LBL-27863).
13. Exploratory Simulations of Multiphase Effects in Gas Injection and Ventilation Tests in an Underground Rock Laboratory by Stefan Finsterle, Erika Schlueter, and Karsten Pruess (NDC-13, LBL-28810).
14. Joint Seismic, Hydrogeological, and Geomechanical Investigations of a Fracture Zone in the Grimsel Rock Laboratory, Switzerland by Ernest L. Majer, Larry R. Myer, John E. Peterson Jr., Kenzi Karasaki, Jane C. S. Long, Stephen J. Martel, Peter Blümling, and Stratis Vomvoris (NDC-14, LBL-27913).
15. Analysis of Hydraulic Data from the MI Fracture Zone at the Grimsel Rock Laboratory, Switzerland by Amy Davey, Kenzi Karasaki, Jane C.S. Long, Martin Landsfeld, Antoine Mensch, and Stephen J. Martel (NDC-15, LBL-27864).
16. Use of Integrated Geologic and Geophysical Information for Characterizing the Structure of Fracture Systems at the US/BK Site, Grimsel Laboratory, Switzerland by Stephen J. Martel and John E. Peterson Jr. (NDC-16, LBL-27912).

Table of Contents

List of Figures vii

List of Tables ix

Abstract xi

1.0. Introduction 1

2.0. Background 3

3.0. Verification of PTST Method 9

4.0. Application of PTST Solution 13

4.1. DST01 at 281.7m 13

4.2. Annealing and Model Uncertainty 17

5.0. Analysis of Swabbing Data 25

6.0. Conclusions 29

7.0. References 31

Appendix A — Plots for Case 7 through Case 108 33

List of Figures

		Page
Figure 2.1.	Slug test type curves after Cooper et al.	5
Figure 2.2.	Termination at 50 percentile for various values of α_1.	6
Figure 2.3.	Plot of h_{wD} as a function of Horner time.	8
Figure 3.1.	Schematic of the model used in the sensitivity study.	10
Figure 3.2.	Results of Case 1 though 6.	12
Figure 4.1.	Test data and numerical simulation results after Belanger et al. (1987).	14
Figure 4.2.	Horner plot of the buildup data from 281.7m.	16
Figure 4.3.	Flow period match with Ramey et al.'s curves.	18
Figure 4.4.	Three different combinations of r_s and K_s matched with data.	19
Figure 4.5.	Test data and numerical simulation results after Belanger et al. (1987).	20
Figure 4.6.	Horner plot of the buildup data from 850m.	22
Figure 4.7.	Finite radius skin model and the DST data from 850m.	23
Figure 5.1.	Pressure vs. time plot in the 1203.2m interval during swabbing.	26
Figure 5.2.	1/q vs. log time plot for the 1203.2m section.	28
Figure A.1.	Results of Case 7 through 12.	34
Figure A.2.	Results of Case 13 through 18.	35

Figure A.3. Results of Case 19 through 24. 36

Figure A.4. Results of Case 25 through 30. 37

Figure A.5. Results of Case 31 through 36. 38

Figure A.6. Results of Case 37 through 42. 39

Figure A.7. Results of Case 43 through 48. 40

Figure A.8. Results of Case 49 through 54. 41

Figure A.9. Results of Case 55 through 60. 42

Figure A.10. Results of Case 61 through 66. 43

Figure A.11. Results of Case 67 through 72. 44

Figure A.12. Results of Case 73 through 78. 45

Figure A.13. Results of Case 79 through 84. 46

Figure A.14. Results of Case 85 through 90. 47

Figure A.15. Results of Case 91 through 96. 48

Figure A.16. Results of Case 96 through 102. 49

Figure A.17. Results of Case 103 through 108. 50

List of Tables

		Page
Table 3.1.	Matrix of parameters for verification of PTST method	11
Table 4.1.	K_s and r_s used in Figure 4.4	21
Table 5.1.	Comparison of time duration and transmissivity values	27

Abstract

Applicability of the PTST technique was verified by conducting a sensitivity study to the various parameters. The study showed that for ranges of skin parameters the true formation permeability was still successfully estimated using the PTST analysis technique. The analysis technique was then applied to field data from the deep borehole in Leuggern, Northern Switzerland. The analysis indicated that the formation permeability may be as much as one order of magnitude larger than the value based on no-skin analysis. Swabbing data from the Leuggern deep borehole were also analyzed assuming that they are constant pressure tests. The analysis of the swabbing data indicates that the formation transmissivity is as much as 20 times larger than the previously obtained value.

1.0. Introduction

Well testing is one of the most important methods for estimating the flow properties of geologic media. This is because well testing is one of the few methods where direct measurements of the flow properties are made. Although well testing methodologies and analysis techniques are originally conceived for porous media, the same methodologies and analysis techniques are often applied in fractured rocks. However, this is not always appropriate because the assumptions made for porous medium well test methodologies and analysis techniques are not always applicable to fractured rocks. For example, in most cases porous medium solutions assume a slab-like horizontal flow geometry. In fractured rocks on the other hand the flow geometry is controlled by the interconnection of fractures and may not be horizontal. Moreover, fractured rocks are usually highly heterogeneous because there is a wide range of permeability for each fracture. Not much is known about the conditions under which the porous medium assumption can be employed for fractured rock under well test conditions and how much error is involved. Therefore care must be taken when analyzing well test data in fractured rocks. Black and Barker (1987) investigated the error involved in using inappropriate assumptions for slug test interpretations. Karasaki (1989) proposed a PTST technique where a slug test is terminated prematurely and the subsequent recovery data is analyzed. Karasaki reported that through the use of the technique one may be able to obtain a more reliable estimate of the average system permeability and confirm the existence of a local heterogeneity near the well. In the present paper a verification of the PTST technique is conducted by examining the sensitivity of the technique to various parameters.

In the later chapter, the PTST analysis technique is applied to the field data furnished by Nagra through Nagra DOE Cooperative project. Nagra has drilled seven deep boreholes in Northern Switzerland as part of the investigation of the feasibility of geologic isolation of

nuclear wastes. The Leuggern borehole is drilled to a depth of 1688.9m penetrating the crystalline basement rock at a depth of 222m. During drilling and after the completion of the borehole numerous hydraulic tests were conducted. Readers interested in the details of the geology and the hydraulic testing are referred to the reports by Nagra (ex. Belanger et al., 1987). Most of the tests conducted are slug tests and their variations such as pulse injection/withdrawal tests and DST tests. The DST data from a couple of intervals are examined by using PTST analysis method and compared to the results of conventional analyses presented in the past literature. Nagra has also conducted series of swabbing tests to sample formation water. In some cases this swabbing data are useful to obtain a more reliable estimate of the formation permeability than the data from short term slug tests. A couple of examples are shown to demonstrate this innovative approach. As a background for this report, the theory behind slug test analysis is briefly discussed in the following section.

2.0. Background

Slug tests were originally developed for estimating flow parameters of shallow aquifers, which are often well approximated as homogeneous porous media. They have also been widely used to estimate the flow parameters of heterogeneous systems such as fractured rocks. The attractiveness of slug tests is that they are inexpensive and easy to perform and require a relatively short time to complete. On the other hand, analyses of slug test results suffer a problem of nonuniqueness, more than other type of well tests especially when skin is present (Karasaki, 1988).

Cooper, Bredehoeft and Papadopulos (1967) presented a solution for the change in water level for a finite radius well subjected to a slug test in a homogeneous medium. The transient water level $h_{w_s}(t_s)$ in the well normalized to the initial water level is:

$$h_{w_s}(t) = \frac{4\alpha}{\pi^2}\int_0^\infty e^{-t_s\mu^2/\alpha}.\frac{d\mu}{\mu[\Phi^2(\mu)+\Psi^2(\mu)]}, \tag{2.1}$$

where

$$h_s = \frac{h-h_i}{h_0-h_i} \tag{2.2}$$

$$t_s = \frac{2\pi Tt}{C_w} = t_D\cdot\alpha \tag{2.3}$$

$$\alpha = \frac{2\pi r_w^2 S}{C_w} \tag{2.4}$$

$$\Phi(\mu) = \mu J_o(\mu) - \alpha J_1(\mu) \tag{2.5}$$

$$\Psi(\mu) = \mu Y_o(\mu) - \alpha Y_1(\mu) \tag{2.6}$$

and T is the transmissivity of the formation, S is the storativity of the formation and C_w is the well bore storage. For an open hole slug test, $C_w = \pi r_a^2$ where r_a is the radius of the delivery pipe. Equation (2.1) can be evaluated to obtain the type curves as shown in Figure 2.1, which can be used to estimate the transmissivity and the storativity by curve matching.

The Cooper et al.'s solution assumes that there is no skin around the well. However, in fractured rocks there may exist regions around the well whose properties are different from those of the overall medium. These skin effects can be caused not only by drilling but by the inherent nature of the fracture system as well. Because the fracture permeability can be considered as a cubic function of the fracture aperture, the fracture permeability is expected to be distributed over a very wide range. Therefore, the particular fractures intersected by a well may cause skin-like effects. Several workers have investigated the effects of skin on observed fluid levels on slug tests (Ramey and Agarwal, 1972; Ramey et al., 1975; Faust and Mercer, 1984; Moench and Hsieh, 1985; Sageev, 1986; and Karasaki, 1989).

Karasaki (1989) proposed a PTST technique, or a DST, where slug a test is terminated prematurely (Figure 2.2). He stated that a more accurate estimate of the formation permeability can be obtained using a PTST than completing a slug test all the way to the end. Using a PTST method the transmissivity can be estimated by:

$$T = \frac{(h_0 - h_t)C_w h_{wD}(10)}{2\pi t_t (h_{10} - h_i)}, \tag{2.7}$$

where the subscript t denotes the shut-in time, h_0 is the initial head, and h_{10} is the head value at $t/(t-t_t) = 10$. A value of unity for $h_{wD}(10)$ can be used in most cases. Otherwise the equation presented in Karasaki (1989) has to be used:

$$h_{wD}(t_D) = \int_0^{\tau} L_\lambda^{-1}\left\{\frac{-\sqrt{p}K_1(\sqrt{p})}{pK_0(\sqrt{p})+\alpha_1\sqrt{p}K_1(\sqrt{p})}\right\} \cdot L_{t_D-\lambda}^{-1}\left\{\frac{K_0(\sqrt{p})}{\sqrt{p}K_1(\sqrt{p})}\right\} d\lambda$$

$$+\int_{\tau}^{t_D} L_\lambda^{-1}\left\{\frac{-\sqrt{p}K_1(\sqrt{p})}{pK_0(\sqrt{p})+\alpha_2\sqrt{p}K_1(\sqrt{p})}\right\} \cdot L_{t_D-\lambda}^{-1}\left\{\frac{K_0(\sqrt{p})}{\sqrt{p}K_1(\sqrt{p})}\right\} d\lambda \tag{2.8}$$

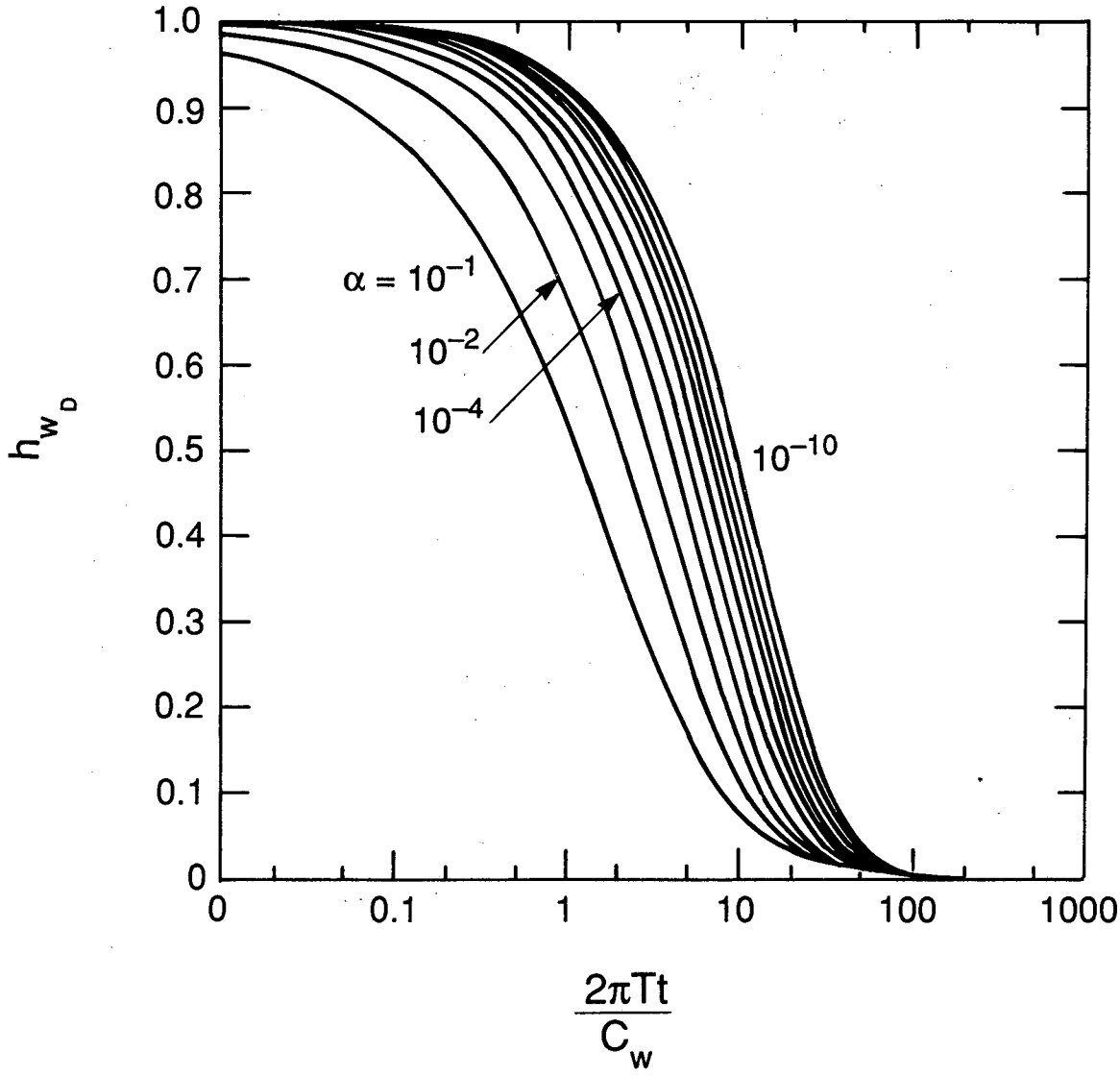

XBL 904 – 6362

Figure 2.1. Slug test type curves after Cooper et al.

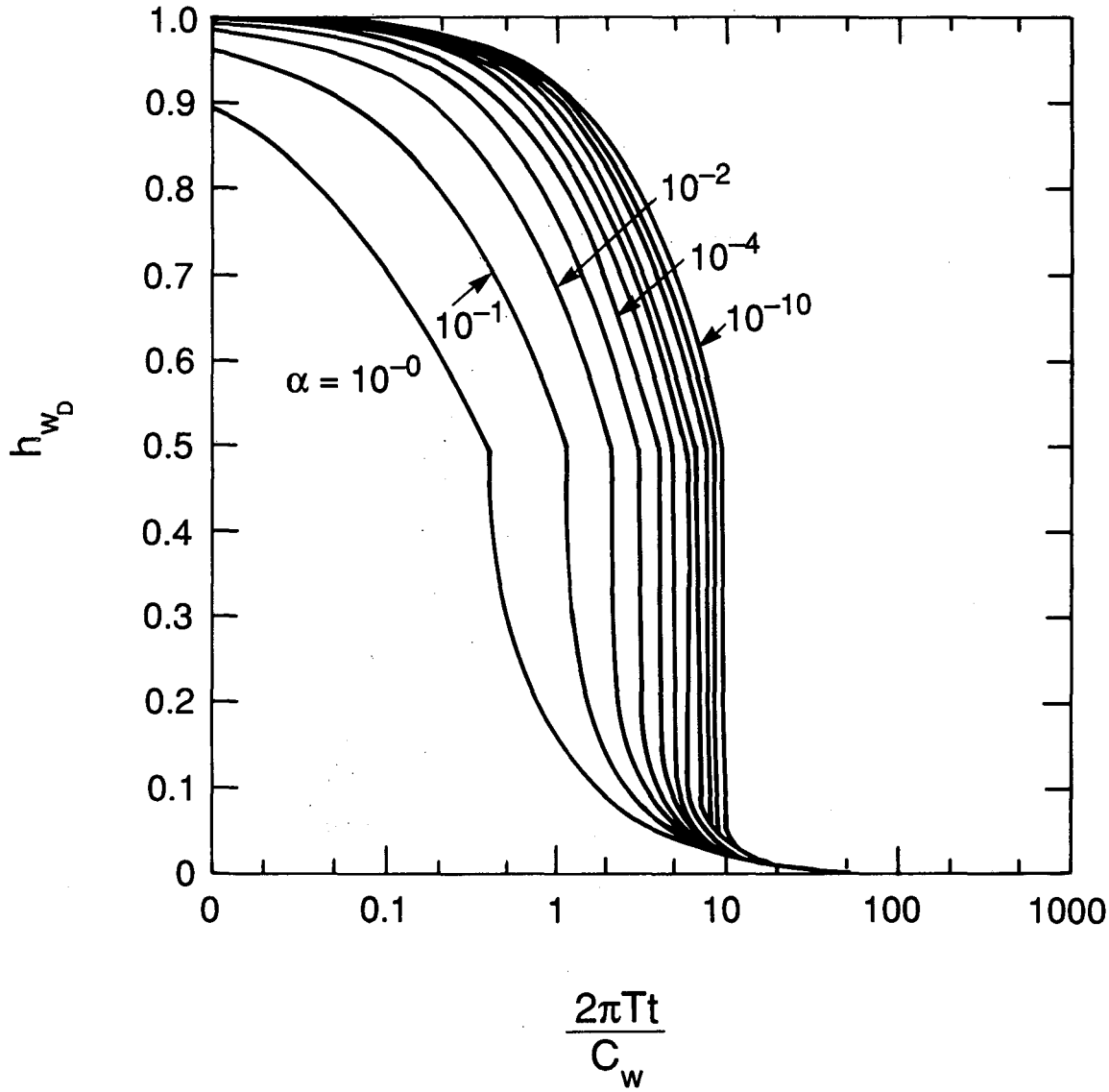

XBL 904 – 6363

Figure 2.2. Termination at 50 percentile for various values of α_1.

where p is the Laplace space variable and L^{-1} denotes Laplace inversion. The subscript denotes the corresponding real space variable. Figure 2.3 shows the plot of h_{wD}.

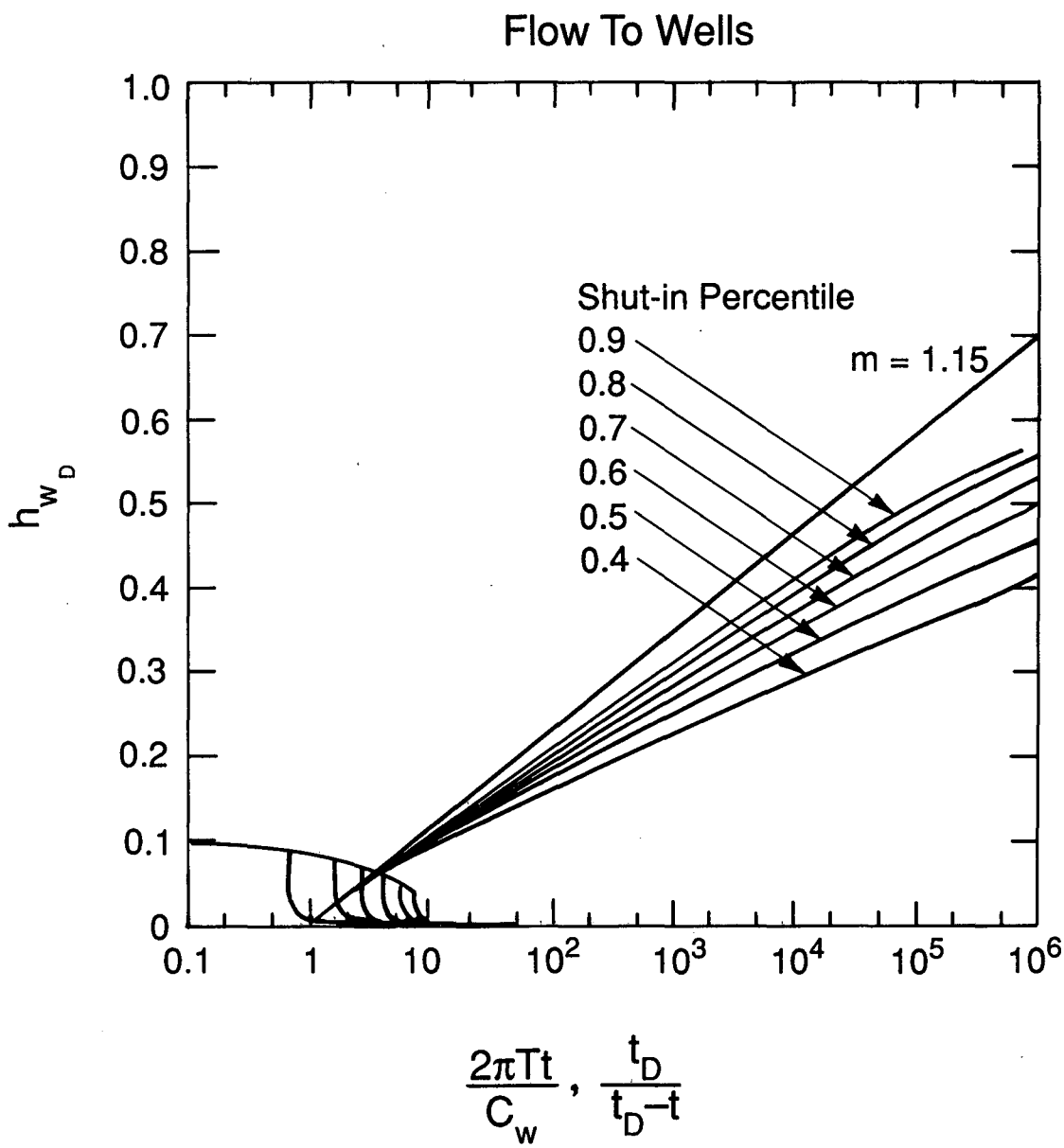

XBL 904 – 6365

Figure 2.3. Plot of h_{wD} as a function of Horner time.

3.0. Verification of PTST Method

To investigate the validity of the PTST method, a sensitivity study was carried out. A PTST was mathematically simulated in a radial composite model where the inner region is a finite radius skin. Figure 3.1 shows the schematic of the model. The parameters varied were the permeability and specific storage of the inner region (skin) and the outer region, the radius of the inner region, and the termination level. Table 3.1 shows the matrix of parameters used for the study. In each case three different skin permeabilities were tested for a given K_2. For $K_2 = 10^{-7}$, the skin permeabilities were $K_1 = 10^{-7}, 10^{-8}, \text{and} 10^{-9}$. For $K_2 = 10^{-8}$, $K_1 = 10^{-8}, 10^{-9}, \text{and} 10^{-10}$. Finally, for $K_2 = 10^{-9}$, $K_1 = 10^{-9}, 10^{-10}, \text{and} 10^{-11}$. C_w is assumed to be 1.0×10^{-3} and the formation thickness b to be 10m. r_s is the dimensionless skin radius, i.e., the ratio of the radius of skin to the wellbore radius. Figure 3.2 shows results from Case 1 though 6. The y axis is $\frac{(h-h_i)t_t}{(h_0-h_t)C_w}$, the normalized head divided by the average flow rate and the x axis is the horner time. Therefore, from Equation (2.7) K_2 can be estimated. The solid line corresponds to the largest skin permeability, the dotted line to the medium and the broken line to the smallest skin permeability. The rest of the results can be found in the Appendix. As can be seen in the figures, in all the cases the correct K_2 value can be estimated.

Therefore, it can be concluded that the PTST technique can be used to estimate a reliable formation permeability in the presence of a skin within the ranges of parameters cited. Temperature effects, borehole pressure history and underdamped cases were not considered in the verification. However, for most groundwater applications these effects are negligible.

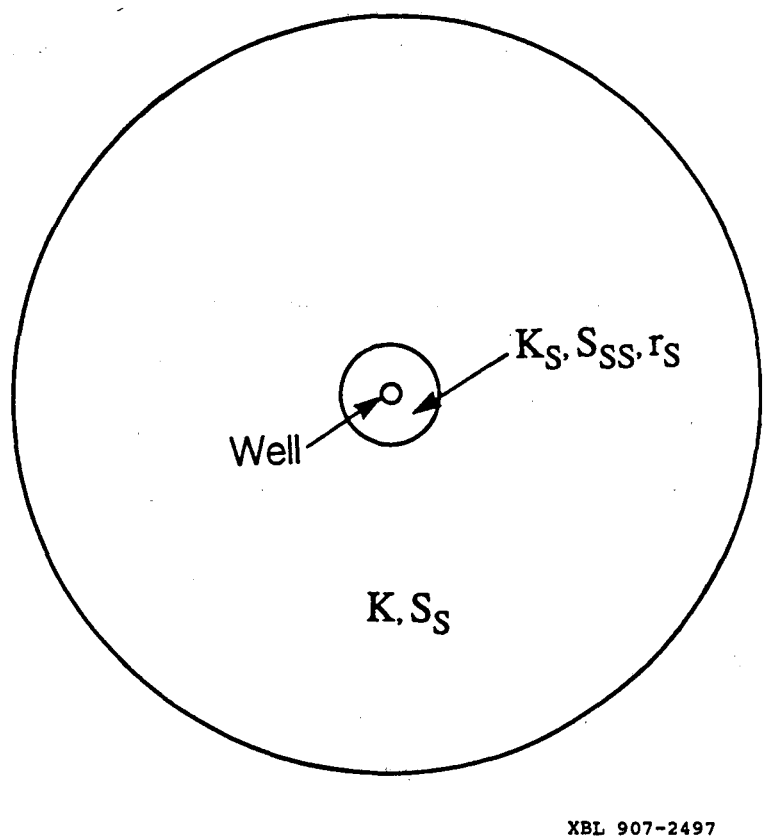

Figure 3.1. Schematic of the model used in the sensitivity study.

Table 3.1. Matrix of parameters for verification of PTST method

K_2	r_s	h_s	.5						.9					
		S_{s2}	10^{-5}		10^{-6}		10^{-7}		10^{-5}		10^{-6}		10^{-7}	
		S_{s1}	10^{-5}	10^{-6}	10^{-5}	10^{-6}	10^{-5}	10^{-6}	10^{-5}	10^{-6}	10^{-5}	10^{-6}	10^{-5}	10^{-6}
10^{-7}	2.0		1	2	3	4	5	6	55	56	57	58	59	60
	1.2		7	8	9	10	11	12	61	62	63	64	65	66
	10.		13	14	15	16	17	18	67	68	69	70	71	72
10^{-8}	2.0		19	20	21	22	23	24	73	74	75	76	77	78
	1.2		25	26	27	28	29	30	79	80	81	82	83	84
	10.		31	32	33	34	35	36	85	86	87	88	89	90
10^{-9}	2.0		37	38	39	40	41	42	91	92	93	94	95	96
	1.2		43	44	45	46	47	48	97	98	99	100	101	102
	10.		49	50	51	52	53	54	103	104	105	106	107	108

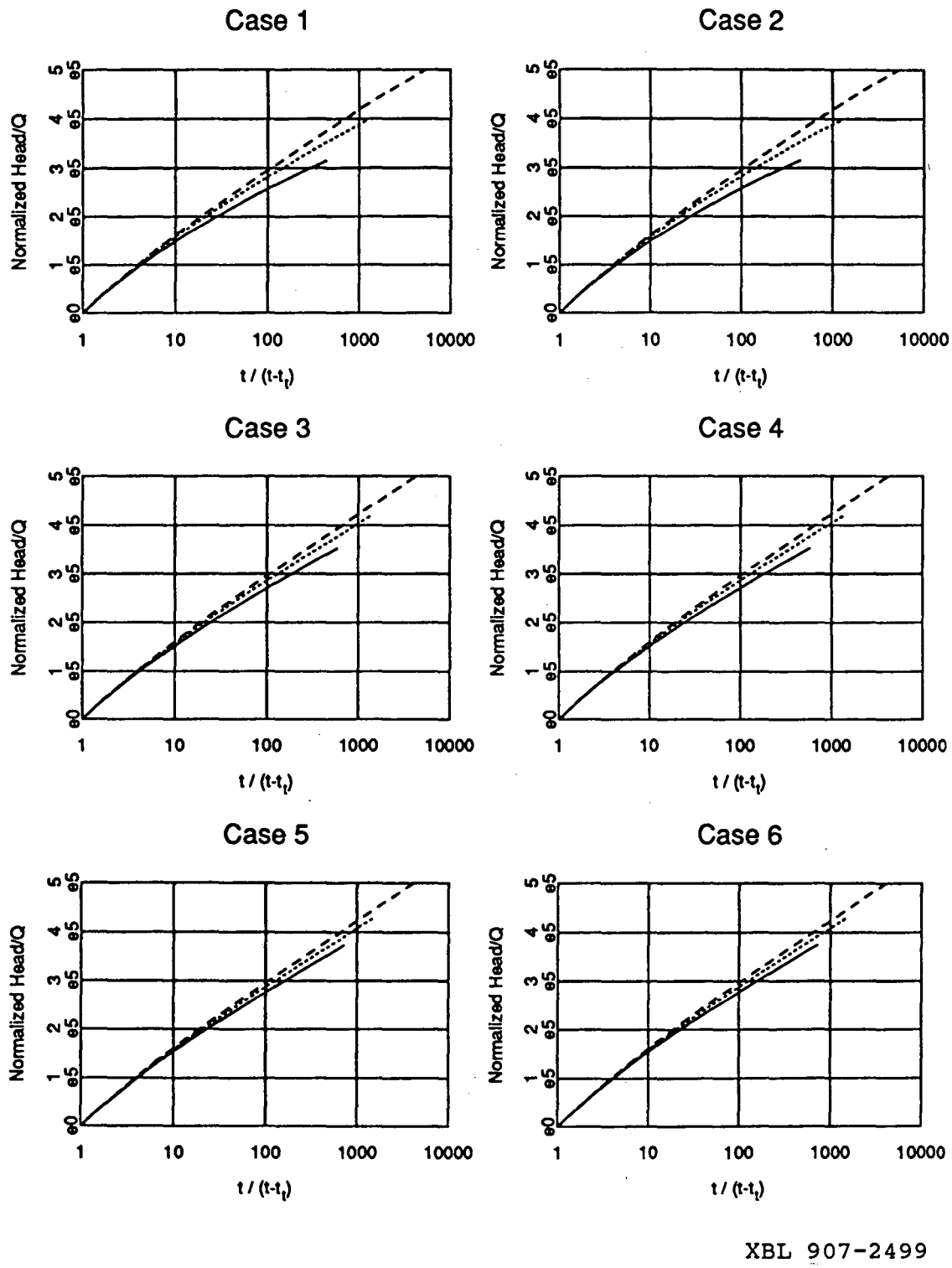

Figure 3.2. Results of Case 1 though 6.

4.0. Application of PTST Solution

In addition to pulse injection/withdrawal tests and slug injection/withdrawal tests, Nagra conducted drill-stem tests (DST's) in several intervals. Although they were not terminated at 50% fluid level as suggested in Karasaki (1989), a similar analysis method can be applied to these data. To demonstrate the application of PTST method, DST data are chosen from two depth intervals for analysis and the results are compared to those by Belanger et al.(1987). The first data are from a depth of 281.7m and the second is from 850m. In both cases analyses based on single medium assumption do not fit the buildup data very well. These two cases, however, show different buildup behaviors. In the former case the buildup curve asymptotically approaches to a Horner straight line from above and the latter from below. PTST analysis suggests that there is a low-permeability skin zone around the well and that the true formation permeability may be much larger.

4.1. DST01 at 281.7m

In this test the interval was shut-in as early as 5% recovery. Figure 4.1 shows the pressure data during the DST and the numerical simulation results by GTFM (Belanger et al., 1987). As can be seen from the figure, reasonably good matches are obtained with the pulse injection/withdrawal data and the flow period data. However, the numerical simulations do not match the shut-in period data very well. A much larger permeability has to be assumed in order to match the fast recovering data. However, a permeability of 6×10^{-9}m/s was chosen for this interval. This is because Belanger et al.'s goal was to find a single permeability that best matches all the data from an interval assuming a homogeneous medium, although the numerical simulator GTFM itself is capable of modeling a heterogeneous medium.

A skin would explain the discrepancy discussed above, i.e., a low permeability model

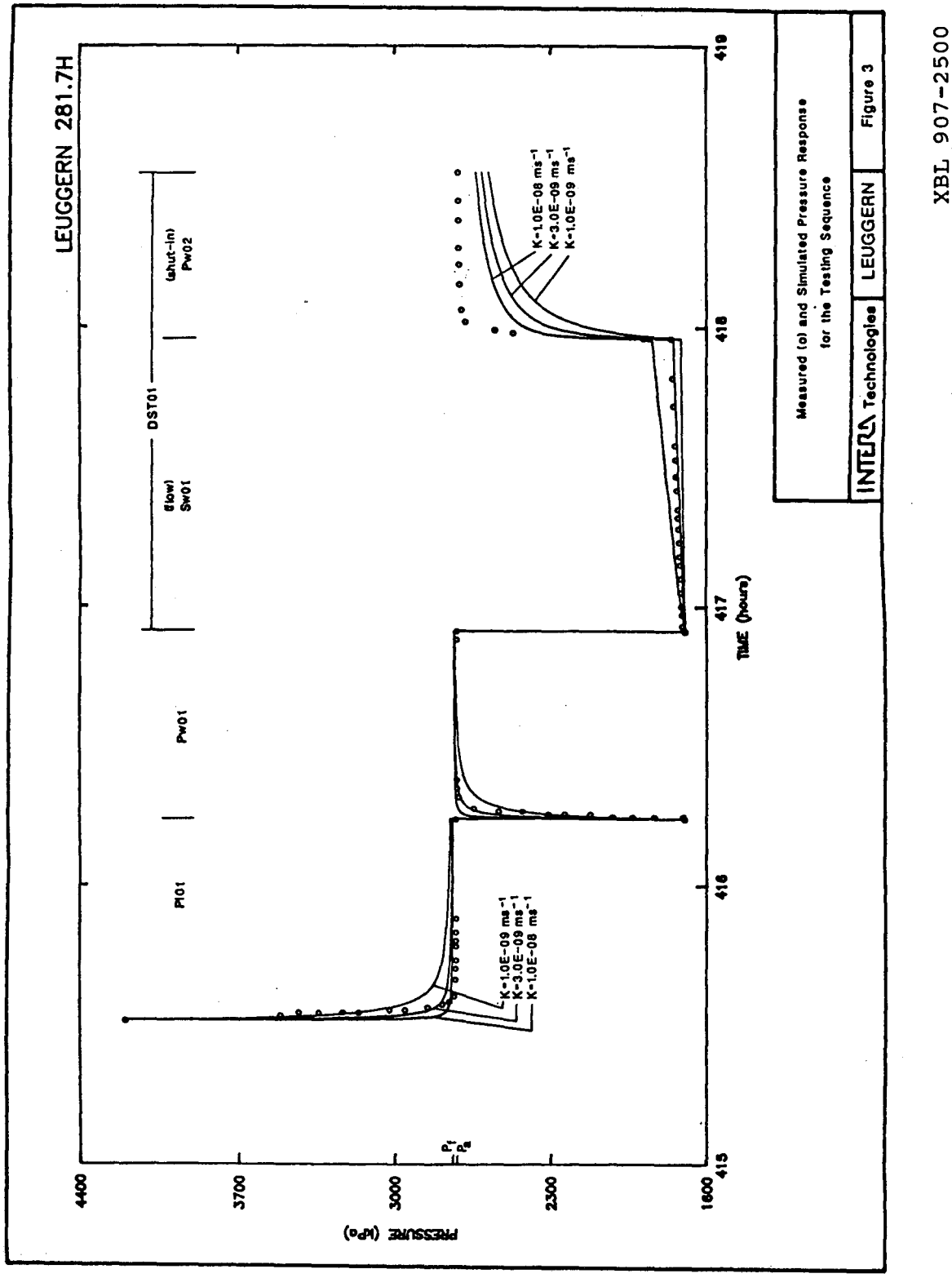

XBL 907-2500

Figure 4.1. Test data and numerical simulation results after Belanger et al. (1987).

matches the pulse injection/withdrawal data and the flow data during the DST, whereas a higher permeability explains the fast recovery after shut-in in DST. Because pulse tests and slug tests (DST flow period) are greatly affected by a low permeability skin (Moench and Hsieh, 1986; Karasaki, 1988), the permeability value obtained by matching those data is probably a closer reflection of the permeability of the skin rather than the medium. The PTST technique calls for the recovery data to be plotted against Horner time (Figure 4.2). As can be seen from the figure, the data asymptotically approach to a straight line from below. In theory, buildup data should approach from above as seen in the next case. The reason for the buildup data approaching from below is suspected that the zone was either re-pressurized when the valve was shut or the shut-in process was not instantaneous. Nontheless, analysis can be attempted. The initial head h_i is 2722Kpa, the head at the start of the test, h_0 is 1696Kpa, and the head at shut-in time, 3800sec is 1760Kpa. The radius of the delivery pipe is 0.05m, and the interval length is 25m. From Figure 4.2, h_{10} is found to be 2703Kpa. Therefore, from Equation (2.7) we obtain:

$$K = \frac{(1696-1760)\text{Kpa}\cdot\pi(0.05)^2\text{m}^2\cdot 1}{2\pi\cdot 25\text{m}\cdot 3800\text{sec}\cdot(2703-2722)\text{Kpa}} = 4.4\times 10^{-8}\text{m/s}$$

This value is about one order of magnitude larger than the previously reported value (Belanger et al., 1987). Next step is to estimate the formation specific storage and the skin parameters, i.e., the skin permeability and the radius. However, when the storativity of the skin is equal to or smaller than that of the formation, which is often the case, it is virtually impossible to estimate these parameters separately from slug tests (Moench and Hsieh, 1986). Only the product αe^{-2s} can be estimated. In theory this could be accomplished by employing Ramey et al.'s analysis alone, where the flow period data is used for type curve matching. However, this is very difficult in many cases because the type curves for intermediate and large values of αe^{-2s} are very similar to each other. In the present case, a unique match would be even more difficult because the slug test was shut-in at a very early stage of the test (95% level). However, from the PTST analysis we already have the estimate of the formation permeability. Therefore, a match point can be calculated from the following equation.

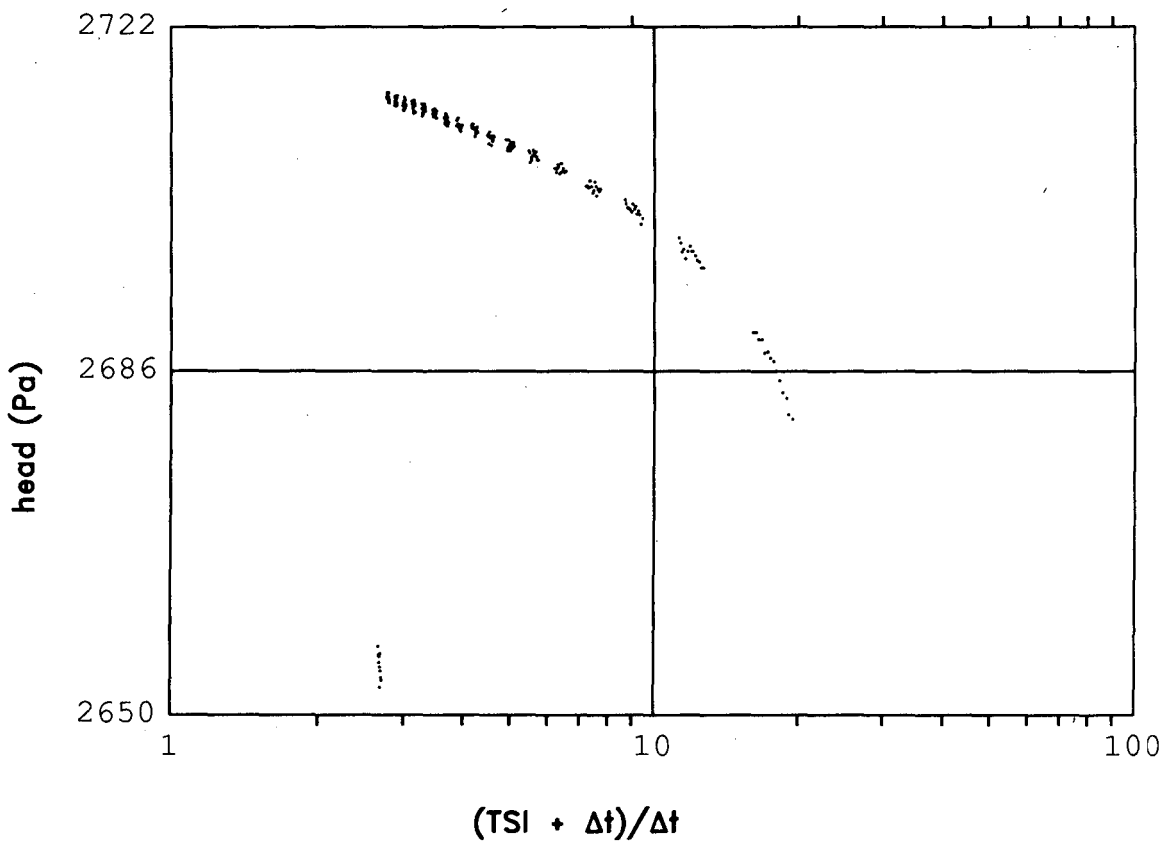

XBL 907-2501

Figure 4.2. Horner plot of the buildup data from 281.7m.

$$t' = \frac{2\pi Tt}{C_w} \tag{4.1}$$

In the present case, $T = 1.1 \times 10^{-6}$ and $C_w = 7.9 \times 10^{-3}$. Therefore, time, t, that corresponds to dimensionless time, t′, equal to, say, unity is 1100seconds. Thus from Figure 4.3, αe^{-2s} is found to be 10^{-55}. In open well tests α generally ranges from 10^{-3} to 10^{-6}. Therefore, a skin coefficient, s, of about 60 is suspected. It is worth recalling here that in most practical cases the curves of Cooper et al. and those of Ramey are identical if the curve label of the former, α is replaced by αe^{-2s}. Therefore, exceptionally small values of α obtained by using Cooper et al.'s analysis are probably αe^{-s} values.

For open well slug tests the skin coefficient, s skin permeability, K_s, formation permeability, K and skin radius, r_s are related by the following equation (Moench and Hsieh, 1986).

$$s = \frac{K}{K_s} \times \ln\frac{r_s}{r_w} \tag{4.2}$$

Therefore, various combinations of r_s and K_s produce similar results. Figure 4.4 shows the data as well as three different combinations of K_s and r_s shown in Table 4.1. As can be seen in the figure all the curves as well as the data fall upon each other. If the skin effect is caused by the drilling the skin radius is expected to be small. On the other hand, skin-like conditions also exist when a borehole intersects a low permeability feature. In such a case the radius can be the size of the feature. If the feature is a low permeability fracture, the skin radius is equivalent to the radius of the fracture. Although in many cases the formation permeability value is of the primary interest, separate estimates of the skin permeability and the radius may be desirable in constructing a detailed model such as a fracture network model. A carefully designed constant flow rate test may be more effective in separating the two parameters (Karasaki, 1986).

4.2. DST01 at 850m

Figure 4.5 shows the pressure data during the DST and the numerical simulation results by GTFM (Belanger et al., 1987). Again the flow period data is not matched very well. The Horner

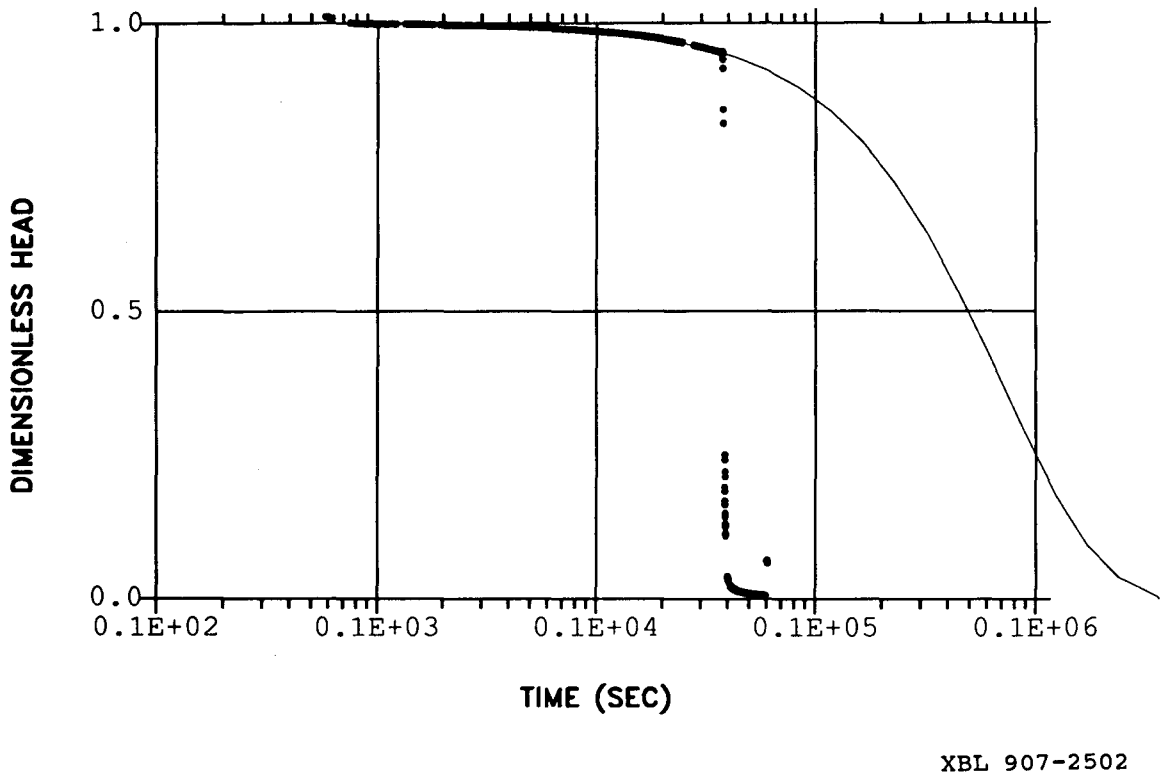

Figure 4.3. Flow period match with Ramey et al.'s curves.

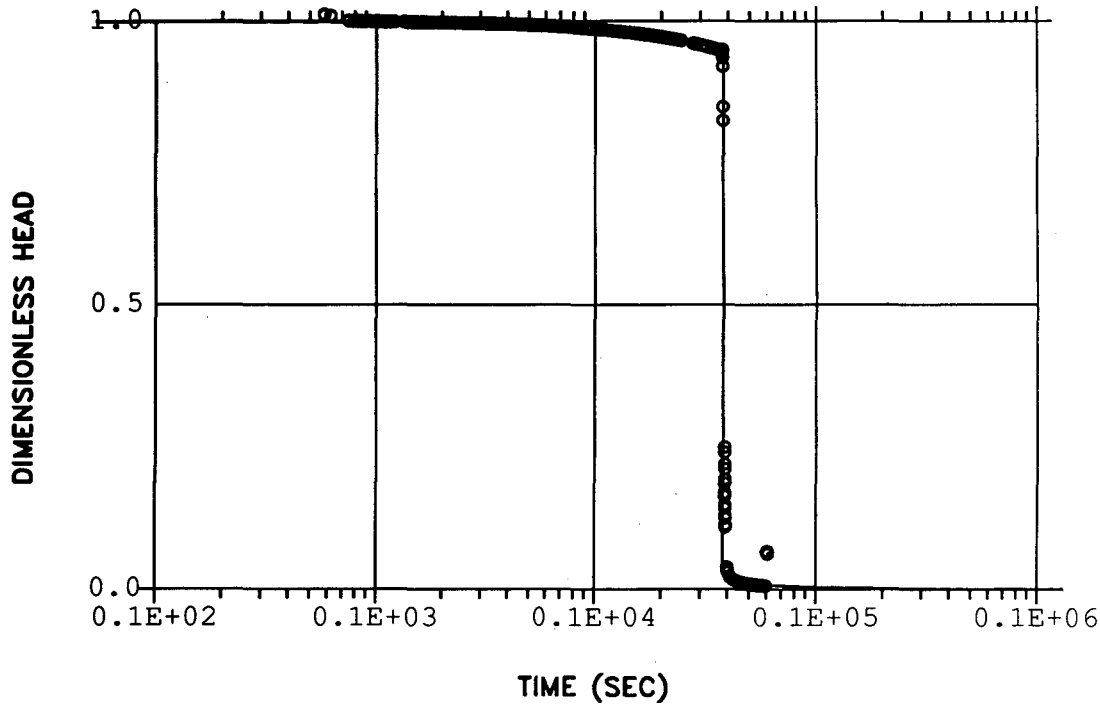

XBL 907-2506

Figure 4.4. Three different combinations of r_s and K_s matched with data.

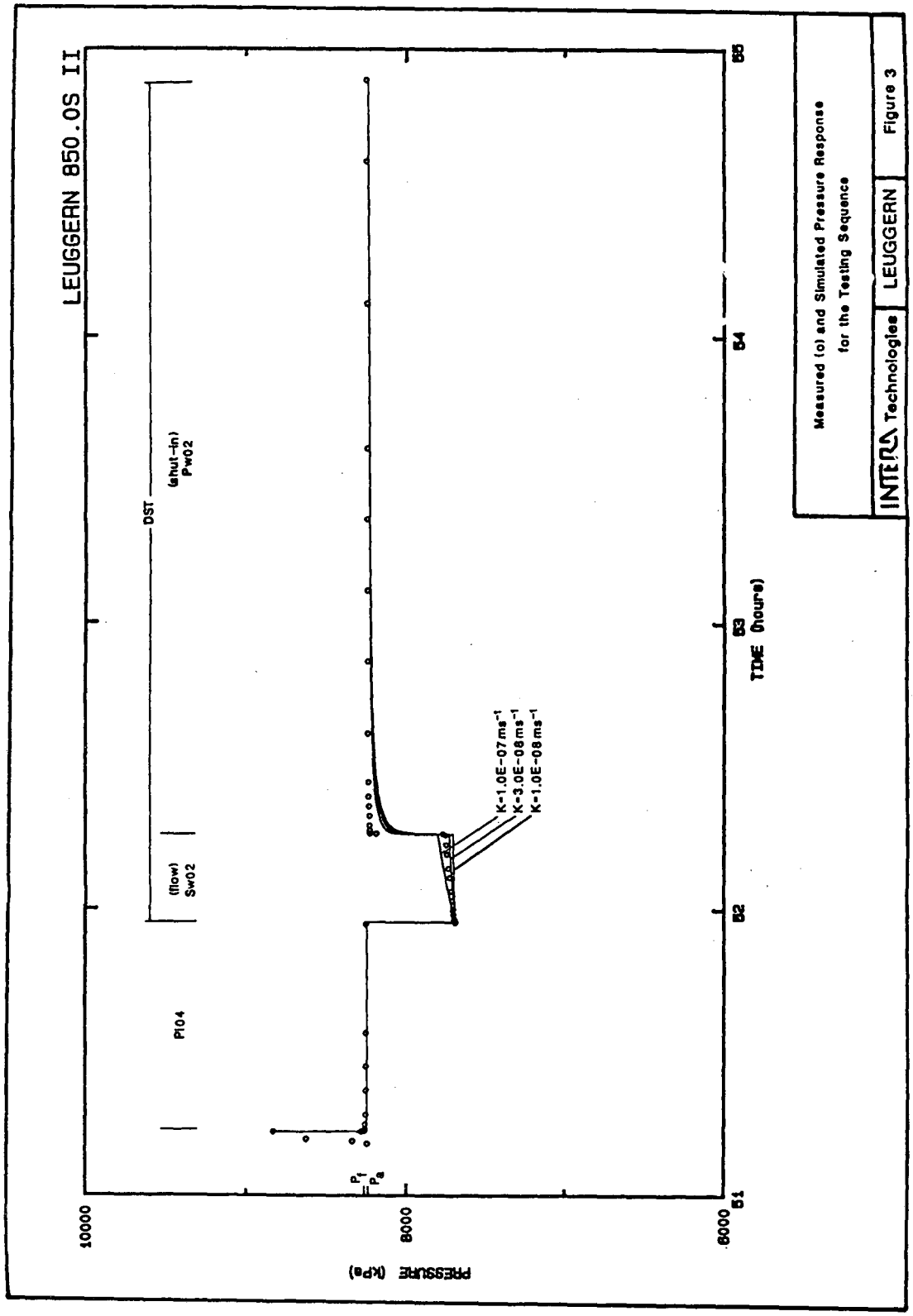

XBL 907-2504

Figure 4.5. Test data and numerical simulation results after Belanger et al. (1987).

Table 4.1. K_s and r_s used in Figure 4.4.

K_s	1.3×10^{-10}m/s	5.0×10^{-10}m/s	1.7×10^{-09}m/s
r_s	1cm	10cm	50cm
S_{ss}	6.9×10^{-7} 1/m		
K	4.4×10^{-8}		
S_s	6.9×10^{-07}		
C_w	7.9×10^{-03}		
b	24.8m		

buildup data is shown in Figure 4.6. As can be seen from the figure, the data asymptotically approach to the straight line from above. Steps similar to those in the previous case can be taken to analyze the data. The initial head h_i is 8256Kpa, the head at the start of the test, h_0 is 7695Kpa, and the head at shut-in time, 1196sec is 7760Kpa. The radius of the delivery pipe is 0.05m, and the formation thickness is 19m. From Figure 4.6, h_{10} is found to be 8220Kpa. Therefore, from Equation (2.7) we obtain:

$$K = 9.9 \times 10^{-8} \text{m/s}$$

The skin coefficient, s is estimated to be 11. The permeability value is comparable to that reported by Belanger et al. However, as can be seen from Figure 4.7, a much better match is obtained assuming a skin.

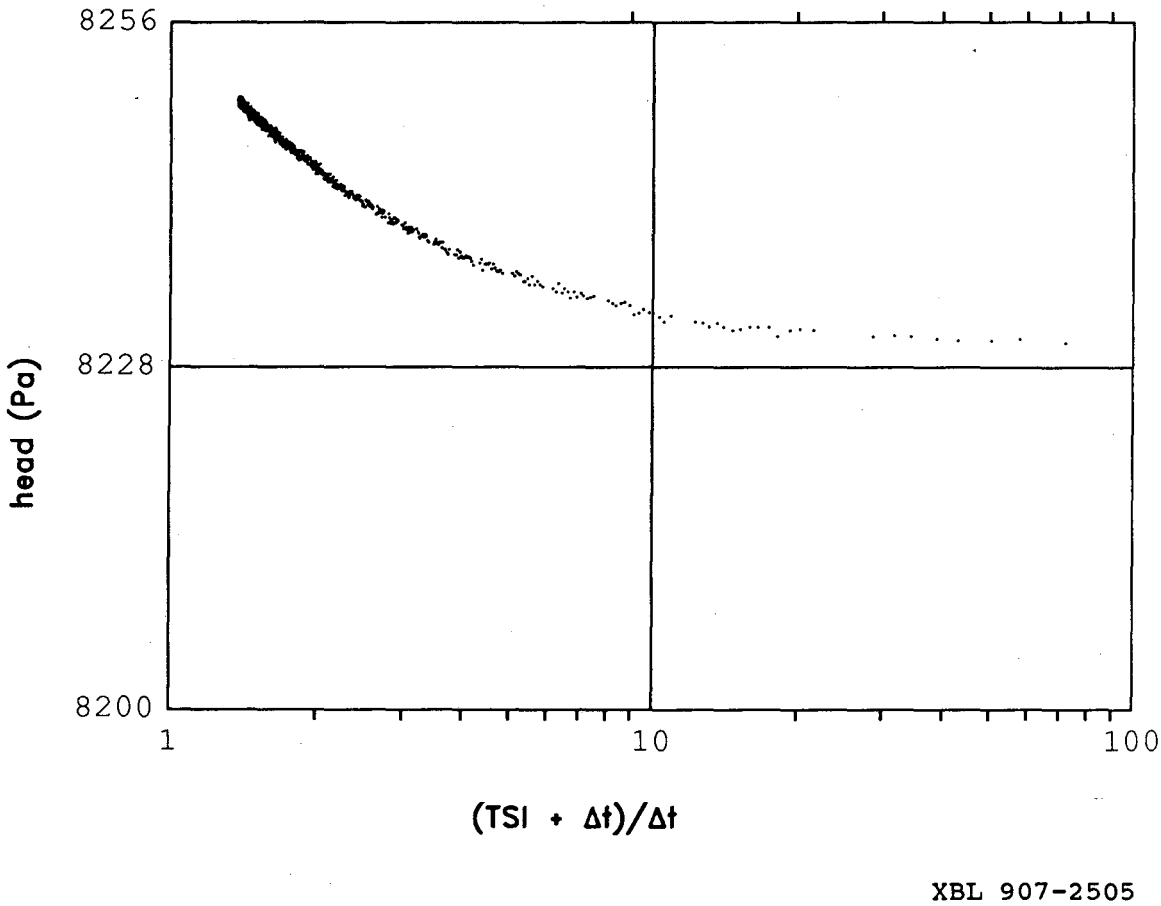

Figure 4.6. Horner plot of the buildup data from 850m.

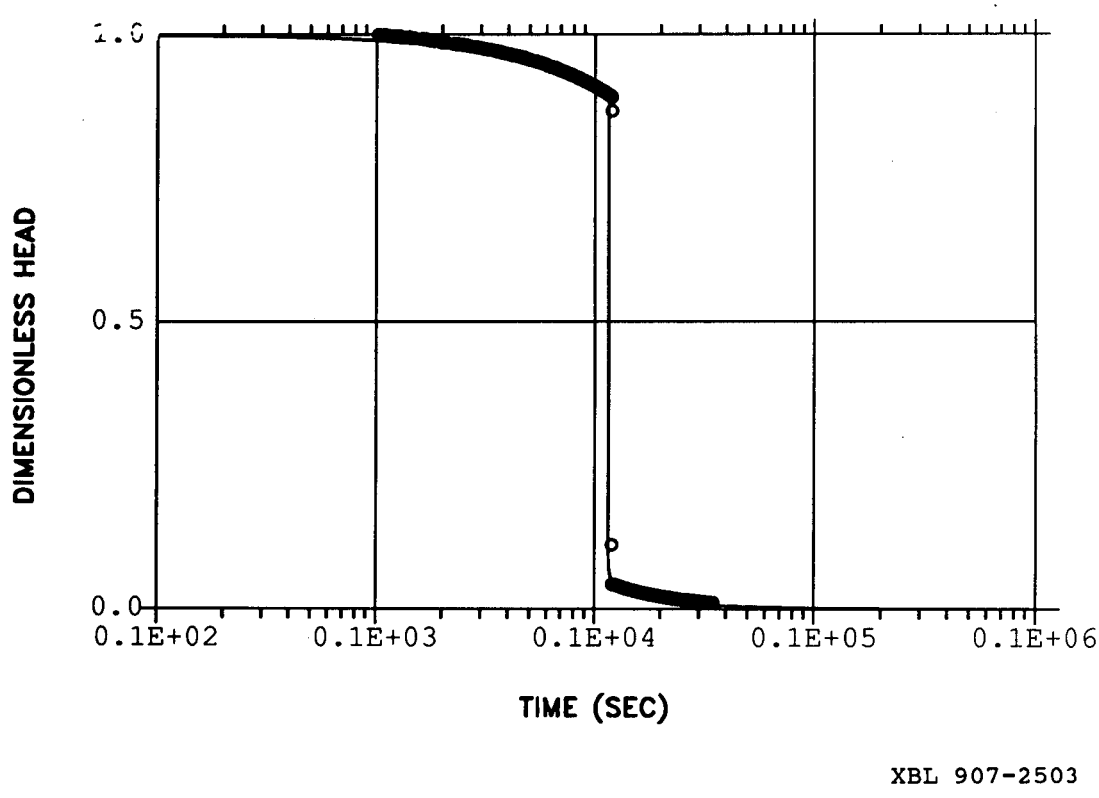

Figure 4.7. Finite radius skin model and the DST data from 850m.

5.0. Analysis of Swabbing Data

Pulse tests and slug tests are very sensitive to the flow properties in the immediate vicinity of the well. The radius of influence is small and the flow properties of a larger volume cannot be uniquely determined. This is because of the nature of the induced boundary condition induced by these tests. For this reason, these tests are not recommended in heterogeneous systems such as fractured rocks. In addition to these short term flow tests Nagra conducted swabbing tests to sample the formation water in the Leuggern borehole. Originally the swabbing was not meant to be part of the hydraulic tests and no attempt to analyze the data during swabbing had been made so far. However, the duration of the swabbing is much greater than any hydraulic tests performed in the zone. For example, in the zone of 1203.2m depth the swabbing lasted almost 26 days as opposed to 14 hours for the pulse withdrawal test, which is the longest hydraulic test. The longer the test duration is, the greater the volume of rock is investigated. In this chapter analysis of swabbing tests are discussed. It is an example how seemingly non-usable data can be made very useful by taking an innovative view.

Swabbing and sampling sequences can be analyzed assuming that they are constant pressure withdrawal tests. This assumption should be adequate when the pressure in the zone is relatively steady and its fluctuation is small compared to the magnitude of the drawdown. Figure 5.1 shows the pressure for the 1203.2m section during the swabbing. It can be seen that although the pressure fluctuates as it responds to each swabbing activity, the magnitude of the fluctuation is small and that overall pressure trend is steady. The flow rate change during each swabbing is expected to be relatively insignificant compared to the overall change in the entire duration. Therefore, the entire duration of the series of swabbing can be conceived as a single constant pressure test. The time duration of the selected swabbing and sampling sequences are two to three orders of magnitude longer compared to other short tests such as pressurized slug and

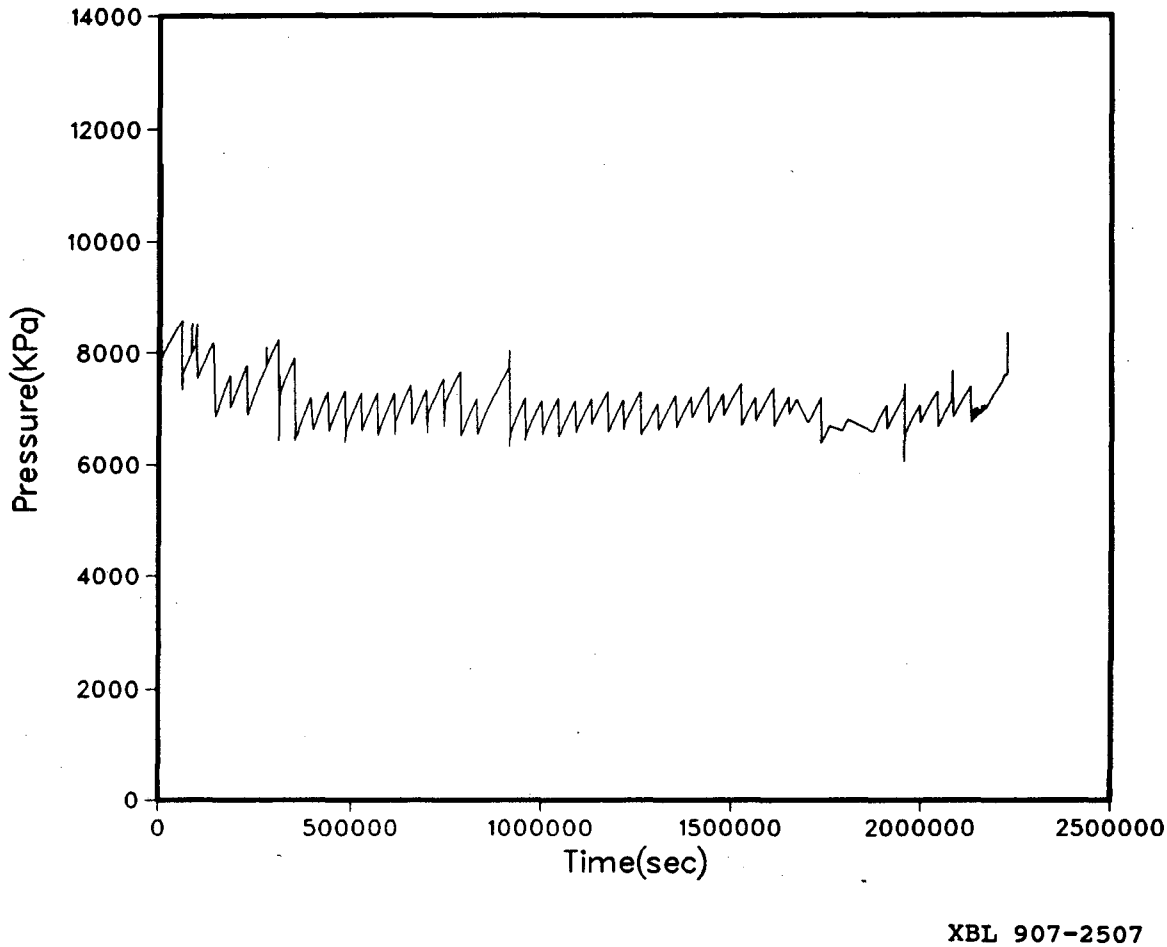

Figure 5.1. Pressure vs. time plot in the 1203.2m interval during swabbing.

open-hole slug tests. For example, the slug test in the 923m zone was in fact a DST test with about 30 minutes of injection and about 1 hour of buildup monitoring. The swabbing and sampling on the other hand lasted more than 270 hours. This means that the volume of rock influenced by the swabbing and sampling sequence is much larger than the slug test. Furthermore, the results of the tests with the constant inner boundary condition (constant pressure) are much more amenable for analysis than those with slug test boundary conditions when wellbore skin and other near-well inhomogeneity is present. Therefore, the resulting flow parameters obtained by analyzing the swabbing and sampling sequences are expected to be more reliable.

Constant pressure drawdown tests can be analyzed by plotting 1/q versus log of time if the test duration is long enough. From the slope of the straight line the transmissivity value can be estimated. The flow rate in this case can be estimated by calculating the volume of water that was taken out at each swabbing based on the pressure decrease in the tubing. Figure 5.2 shows the 1/q vs. log time plot for the 1203.2m section. Table 5.1 shows the comparison of the transmissivity values obtained by analyzing the swabbing and sampling sequences and those obtained by analyzing the slug (pulse) tests (after Belanger et al., 1987) for 923m and 1203m.

Table 5.1. Comparison of time duration and transmissivity values

	Slug Tests		Swabbing & Sampling	
Depth	Duration (hr)	T (m^2/sec)	Duration (hr)	T (m^2/sec)
923m	~1	4.8×10^{-10}	~270	9.2×10^{-9}
1203m	~1	4.8×10^{-9}	~250	5.5×10^{-9}

The analysis of the swabbing data indicates that the formation transmissivity at a depth of 923m is about 20 times larger than the value previously obtained by analyzing the short time pressure tests. The author believes that the value based on the swabbing data analysis is more reliable.

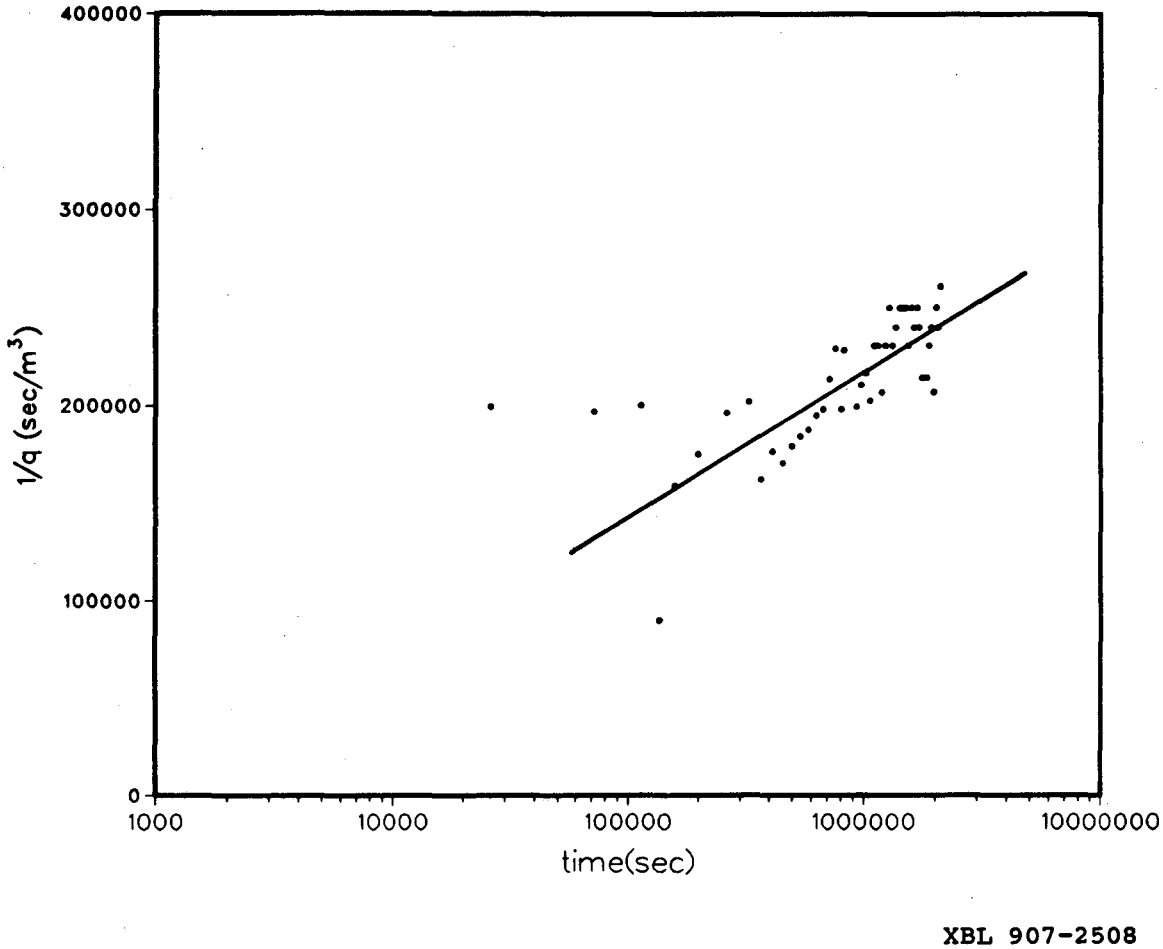

Figure 5.2. 1/q vs. log time plot for the 1203.2m section.

6.0. Conclusions

Applicability of the PTST technique was verified by conducting a sensitivity study to the various parameters. The study showed that for ranges of skin parameters the true formation permeability was still successfully estimated using the PTST analysis technique. The analysis technique was then applied to the field data from the deep borehole in Leuggern, Northern Switzerland. The analysis indicated that the formation permeability may be as much as one order of magnitude larger than previously thought. In a fractured rock skin-like conditions can exist when a borehole intersects a low permeability feature. Therefore, it is important to always recognize the possibility of the existence of a skin.

Seemingly non-usable data can sometimes be made very useful by taking an innovative view. Swabbing data from the Leuggern deep borehole were analyzed assuming that they are constant pressure tests. The analysis of the swabbing data indicates that the formation transmissivity at a depth of 923m is about 20 times larger than the value previously obtained by analyzing the short term pressure tests. The author believes that the value based on the swabbing data analysis is more reliable.

The author recommends not to use slug tests in fractured rocks. Long term pumping tests are believed to be much more reliable. However, if slug tests must be used, it is recommended that the test be terminated at 50% level and that the recovery data be analyzed using the PTST technique.

7.0. References

Belanger, D. W., R. A. Freeze, J. L. Lolcama, and J. F. Pickens, 1987. Interpretation of Hydraulic Testing in Crystalline Rock at the Leuggern Borehole, Appendices Discribing Test Analyses, Nagra Technical Report NIB 87-17.

Cooper, H. H., Jr., J. D. Bredehoeft, and I. S. Papadopulos, 1967. "Response of a Finite Diameter Well to an Instantaneous Charge of Water," *Water Resour. Res., 3,* 263-269.

Faust, C. R., and J. W. Mercer, 1984. "Evaluation of Slug Tests in Wells Containing a Finite Radius Skin," *Water Resour. Res., 20* (4), 504-506.

Karasaki, K., 1986. Well Test Analysis in Fractured Media, Ph.D. Thesis, LBL-21442, April.

Karasaki, K., J. C. S. Long, and P. A. Witherspoon, 1988. "Analytical Models of Slug Tests," *Water Resour. Res., 24* (1), 115-126, January.

Karasaki, K., 1989. "Prematurely Terminated Slug Tests" paper subitted to *Water Resour. Res.*

Moench, A. F. and P. A. Hsieh, 1985. "Evaluation of Slug Tests in Wells Containing a Finite-thickness Skin," *Water Resour. Res., 21* (9), 1459-1461.

Ramey, H. J., Jr. and R. G. Agarwal, 1972. "Annulus Unloading Rates as Influenced by Wellbore Storage and Skin Effect," *Trans.,* A. 453-462.

Ramey, H. J., Jr., R. G. Agarwal, and I. Martin, 1975. "Analysis of 'Slug Test' or DST Flow Period Data," *J. Can. Pet. Tech.,* 37-47.

Sageev, A., 1986. "Slug Test Analysis," *Water Resour. Res., 22* (8), 1323-1333.

Appendix A

Plots for Case 7 through Case 108

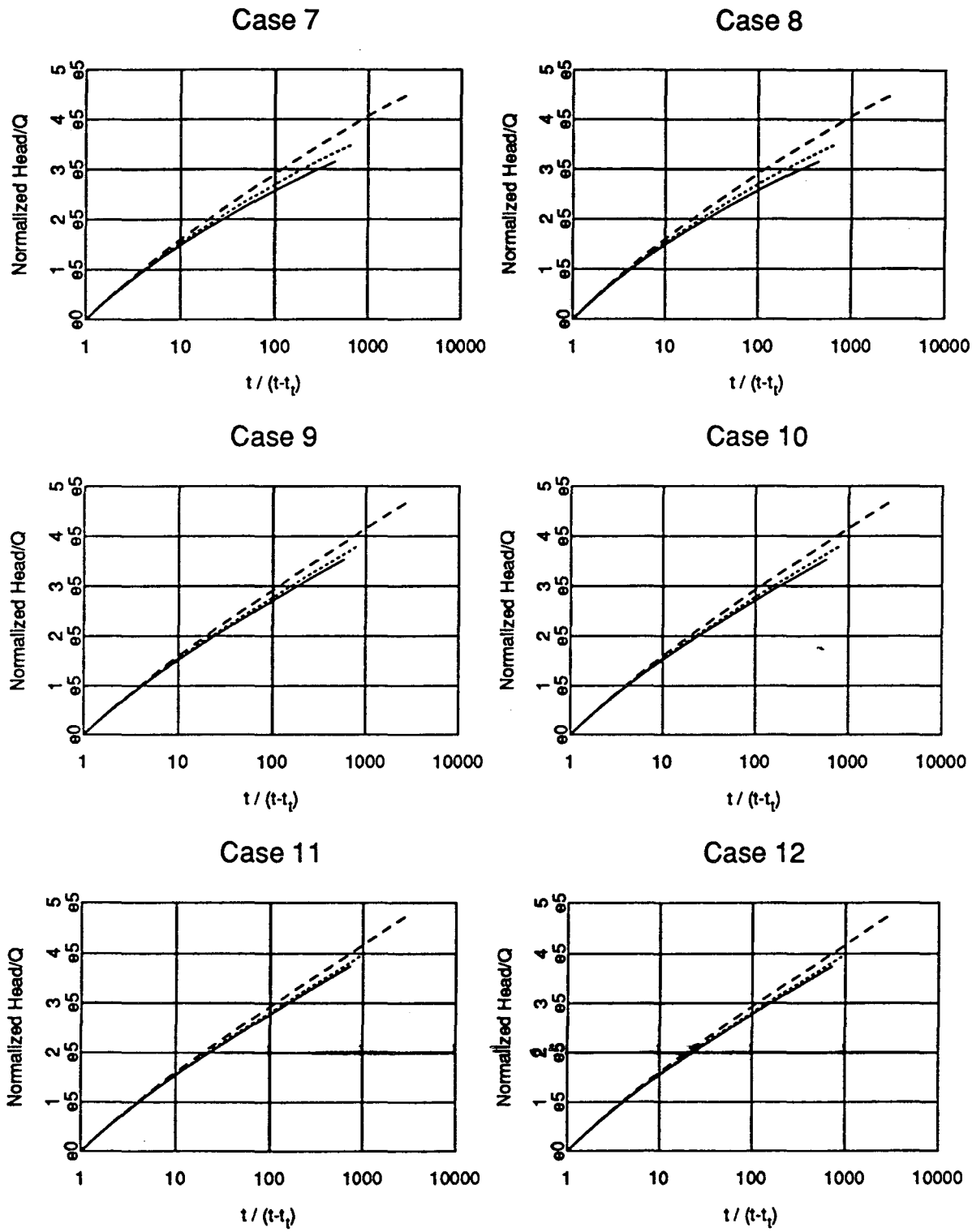

Figure A.1. Results of Case 7 through 12.

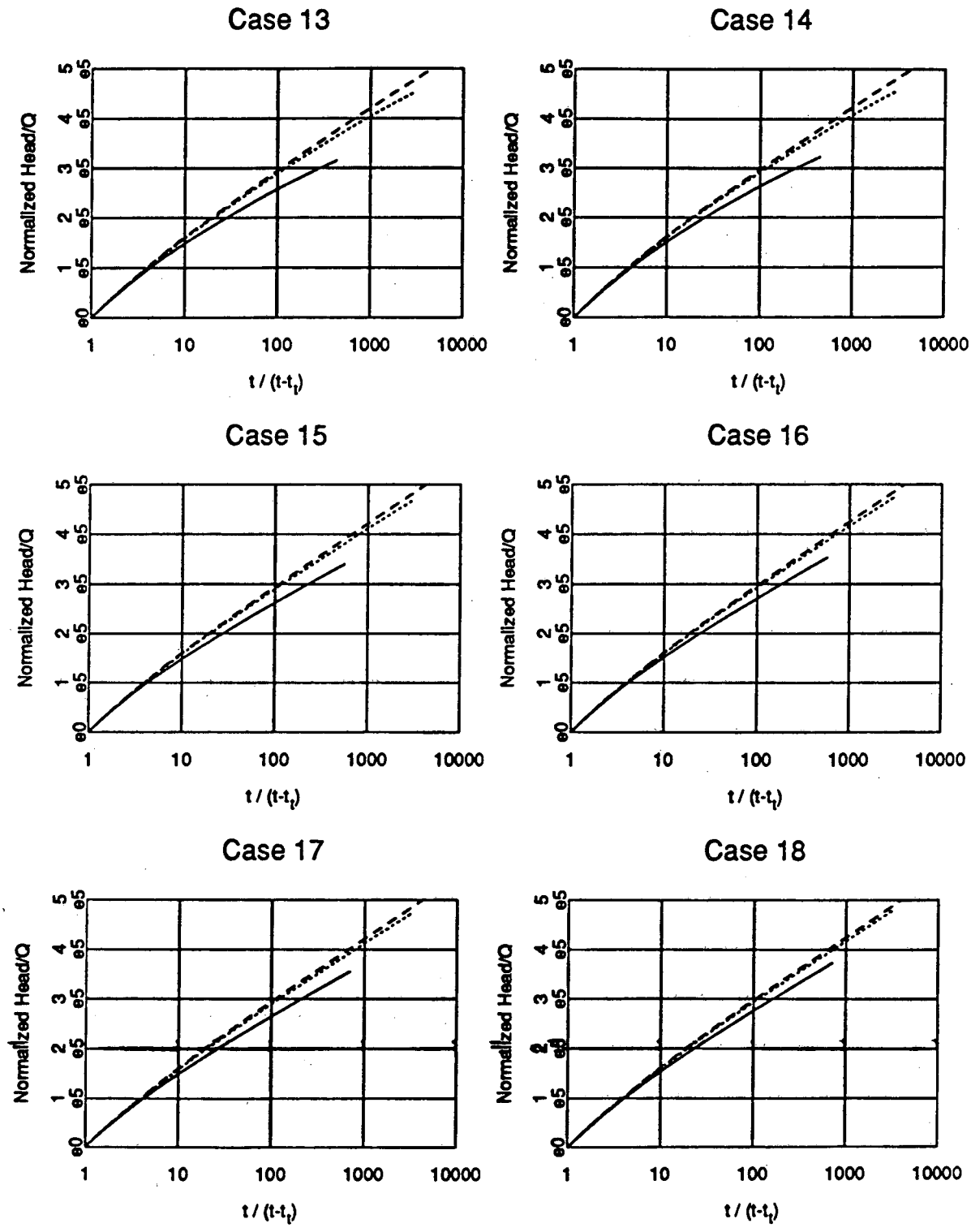

Figure A.2. Results of Case 13 through 18.

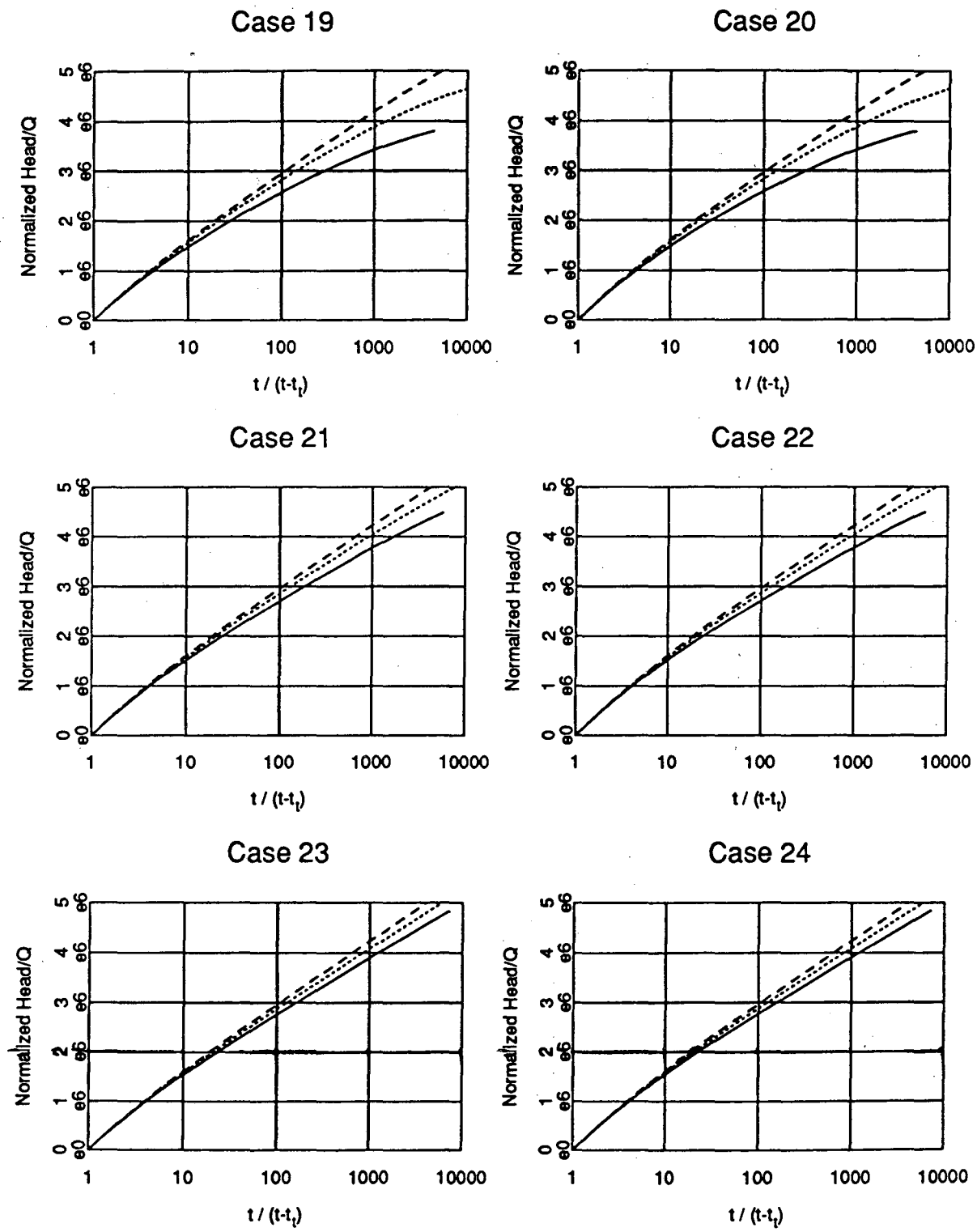

Figure A.3. Results of Case 19 through 24.

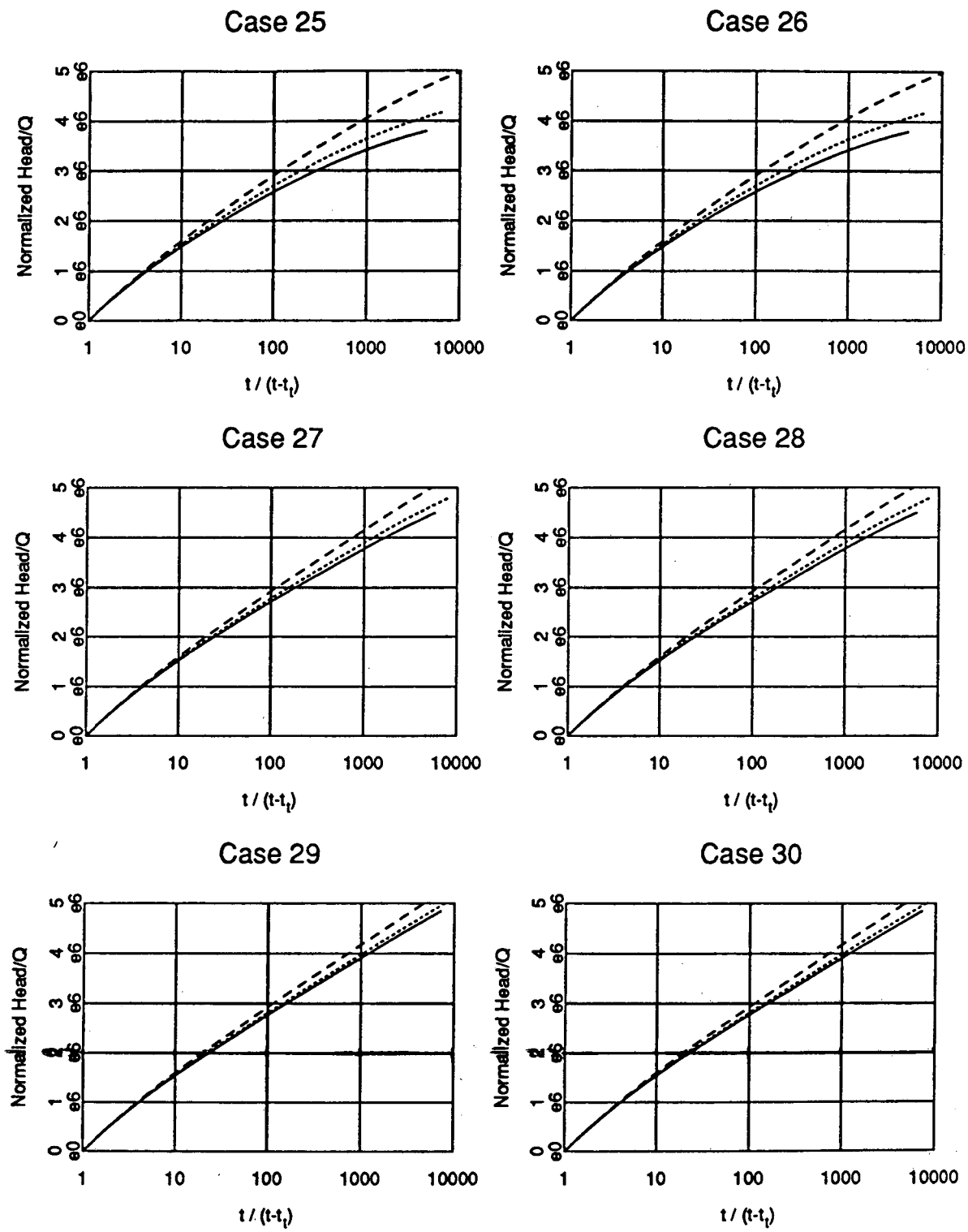

Figure A.4. Results of Case 25 through 30.

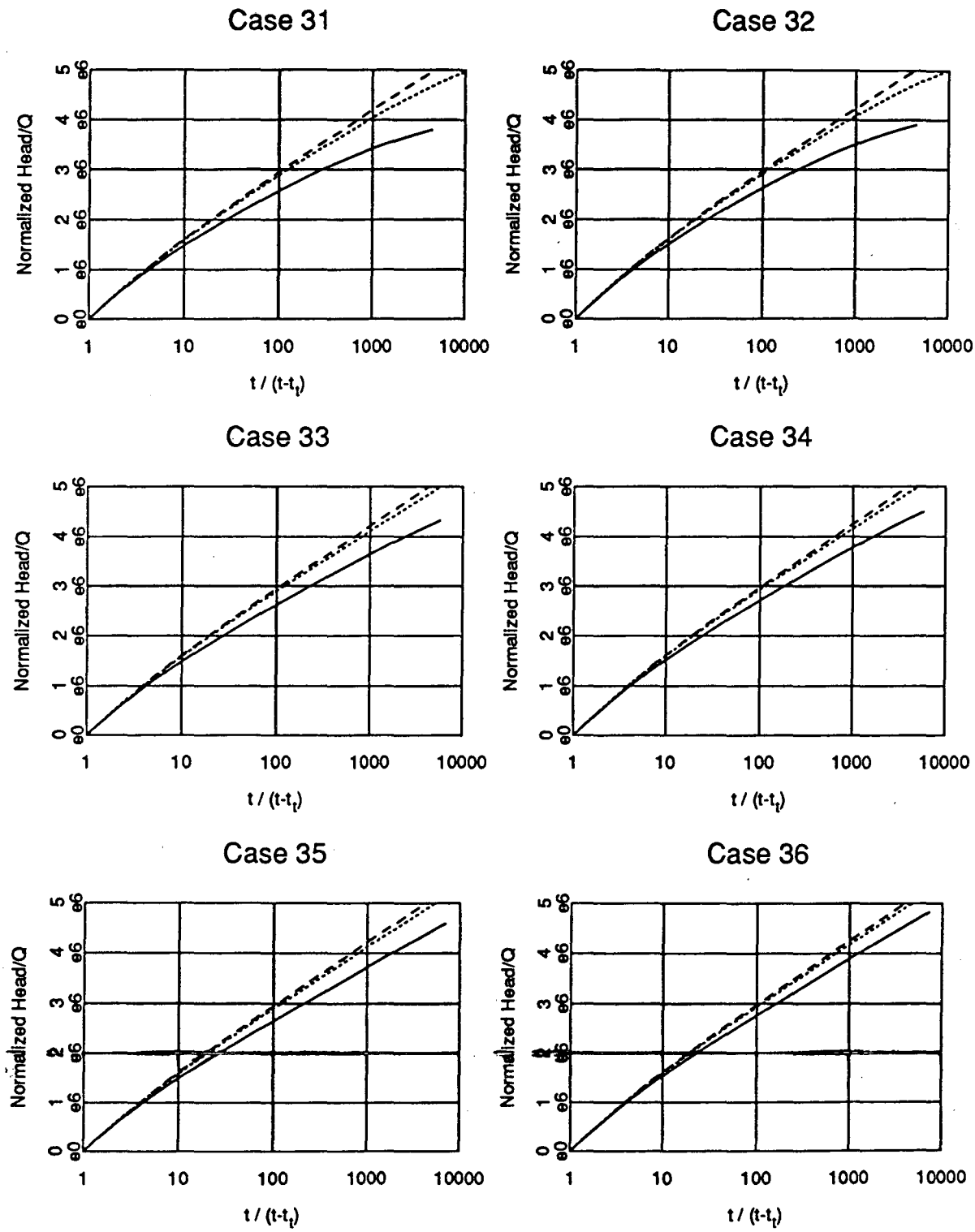

Figure A.5. Results of Case 31 through 36.

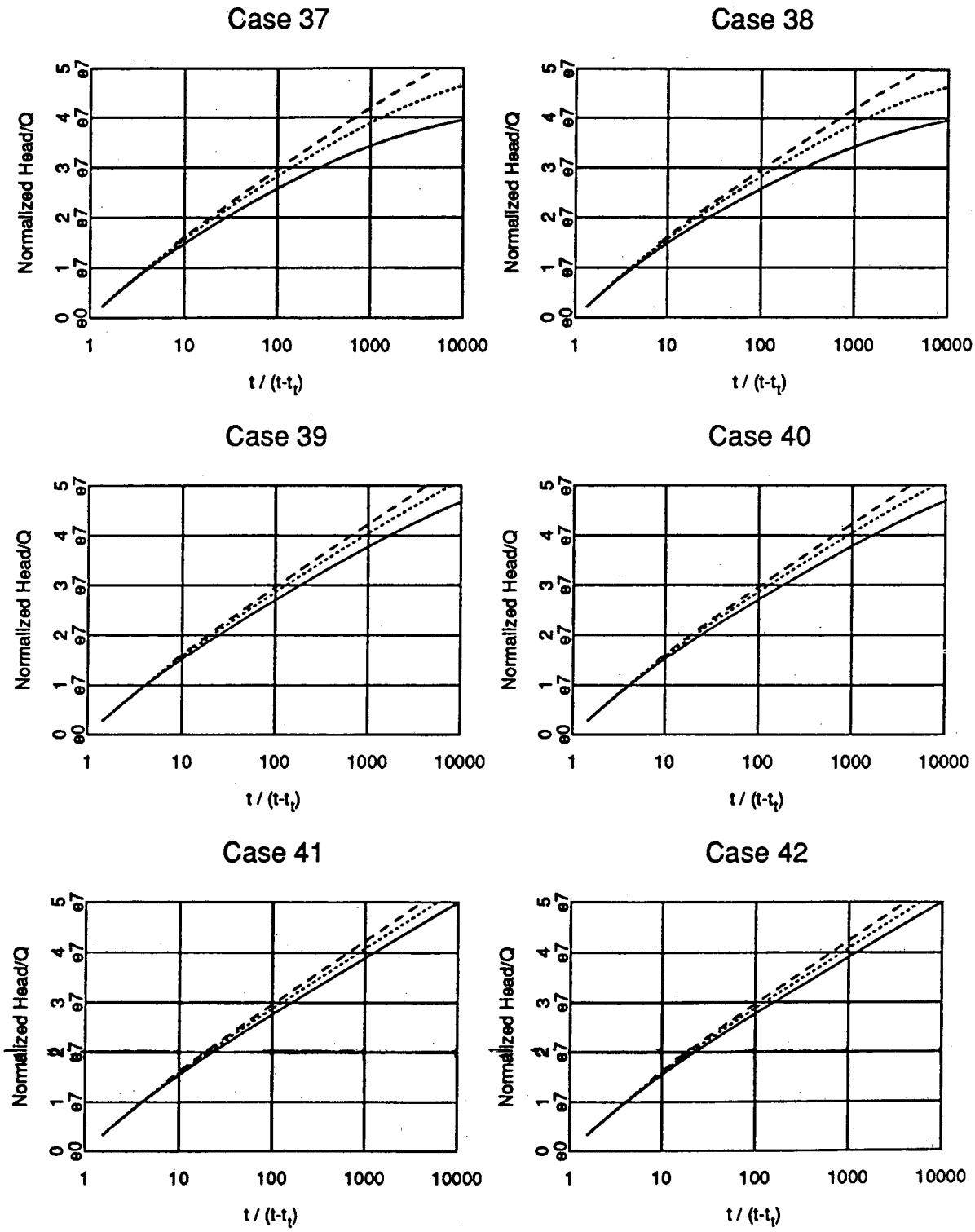

Figure A.6. Results of Case 37 through 42.

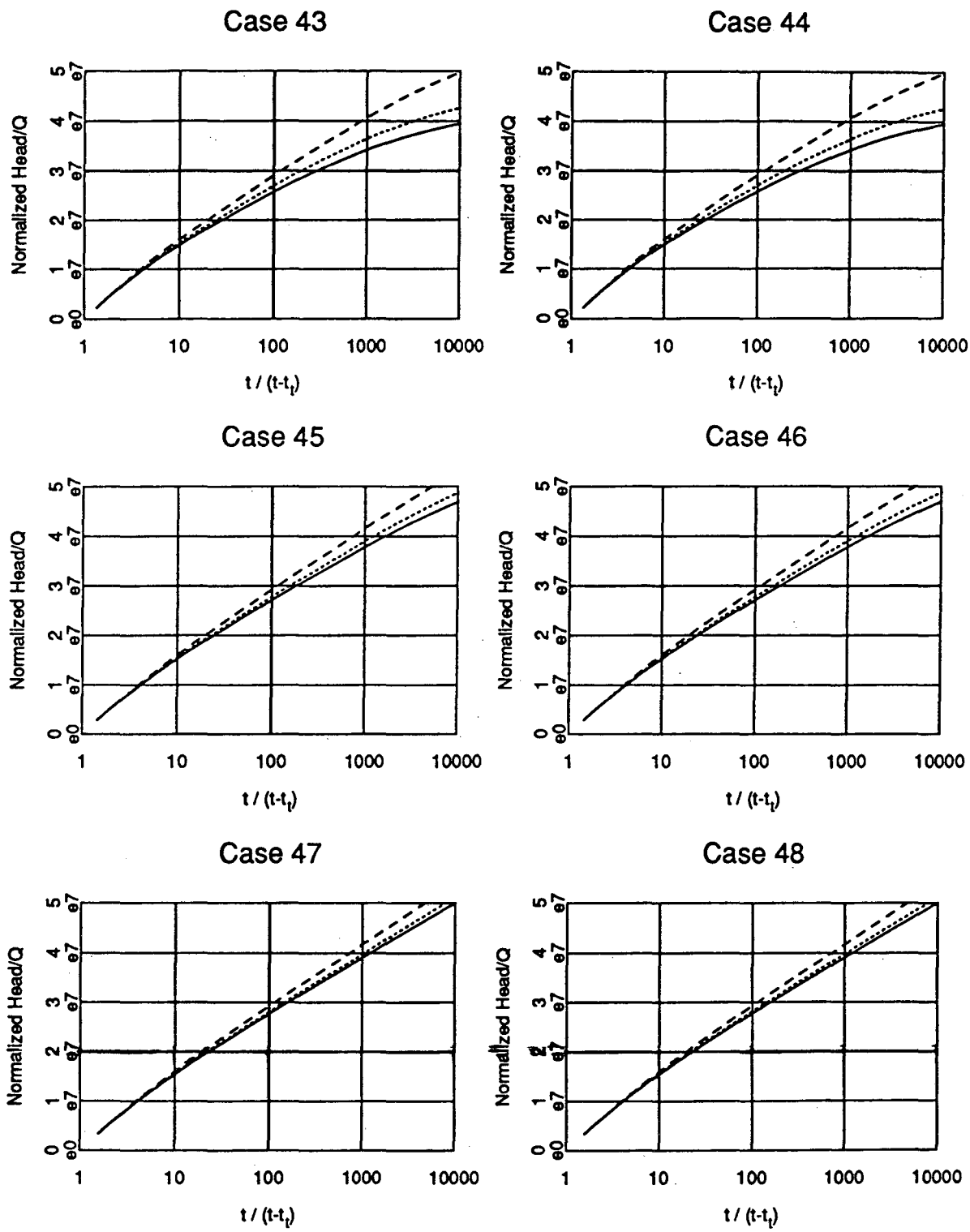

Figure A.7. Results of Case 43 through 48.

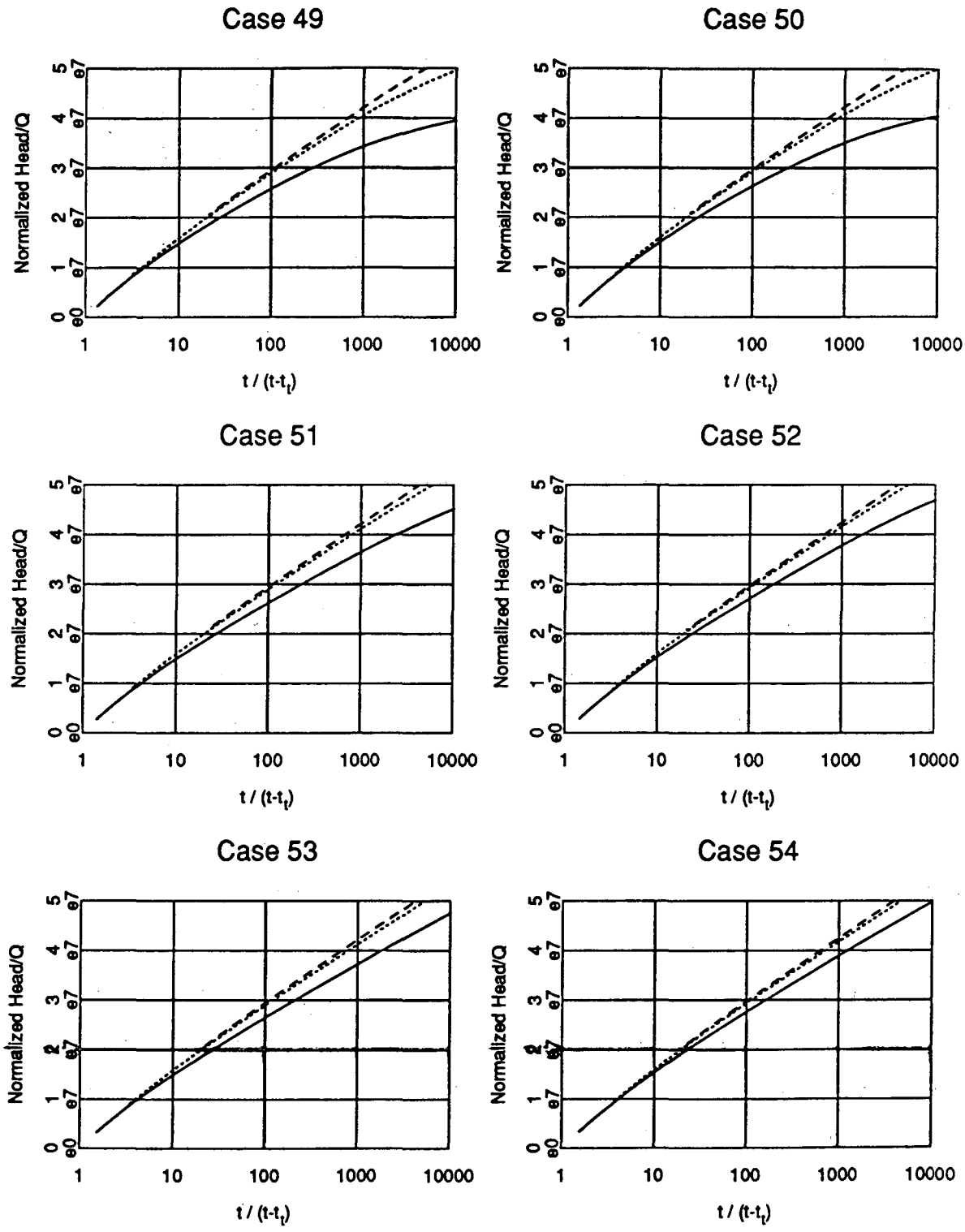

Figure A.8. Results of Case 49 through 54.

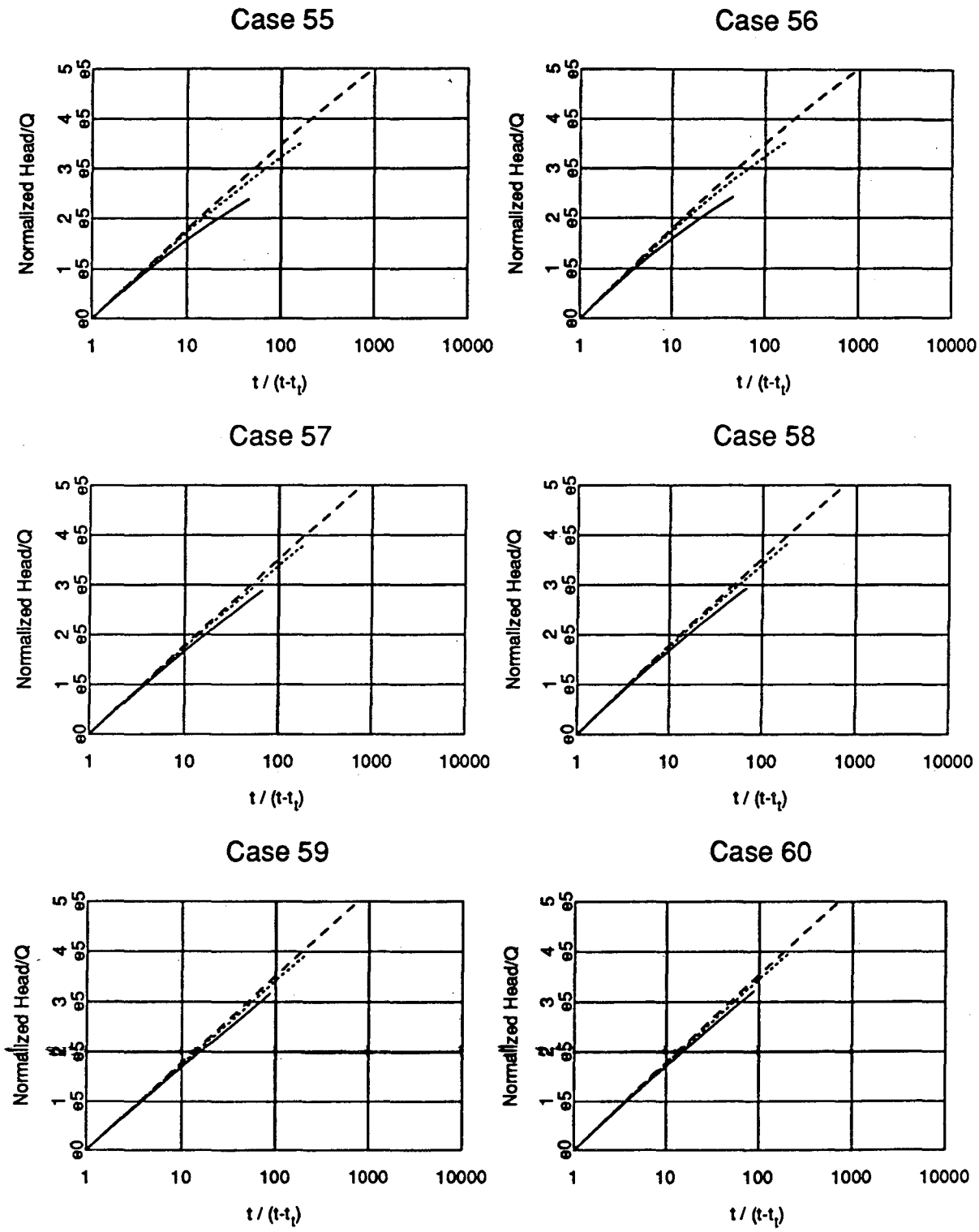

Figure A.9. Results of Case 55 through 60.

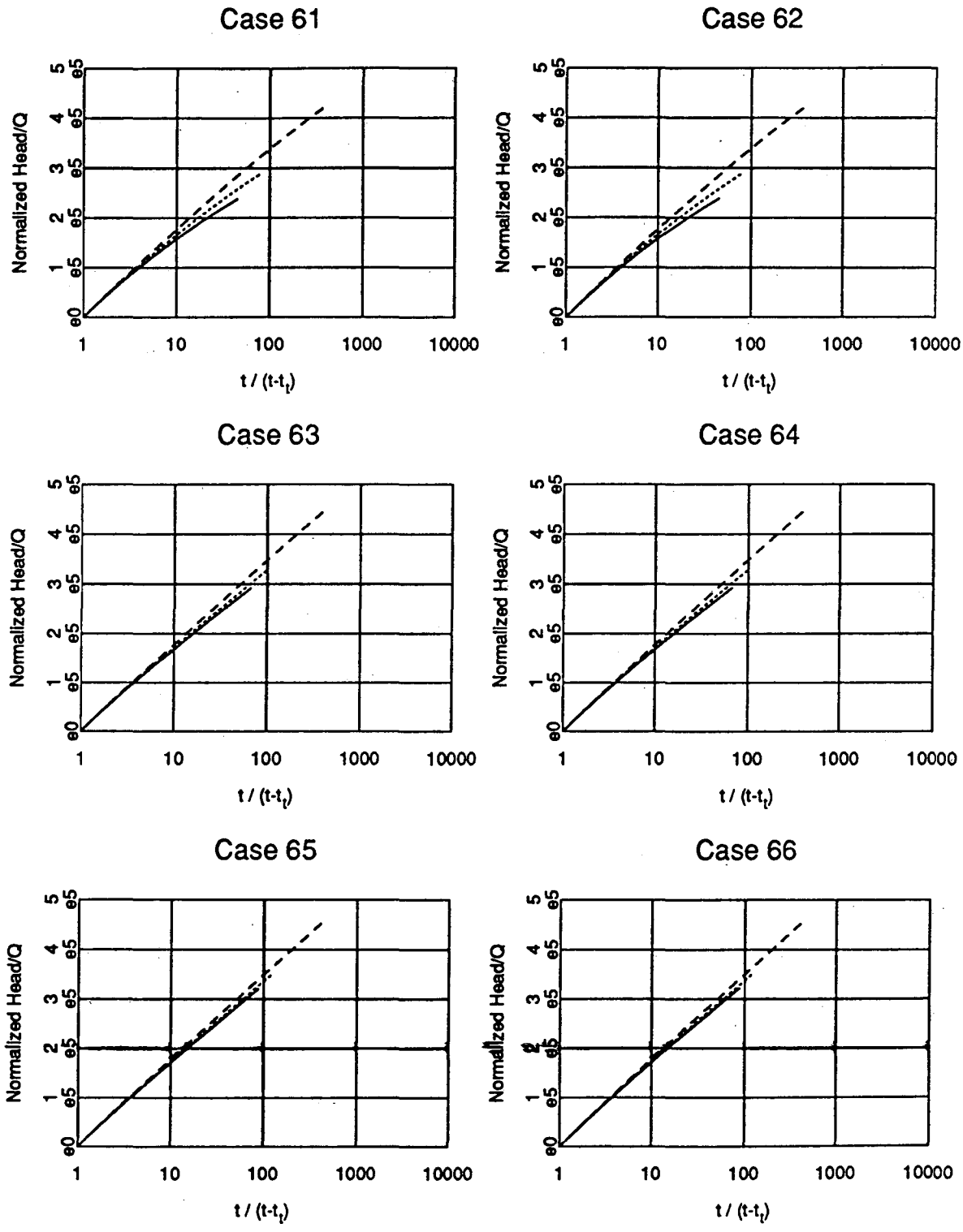

Figure A.10. Results of Case 61 through 66.

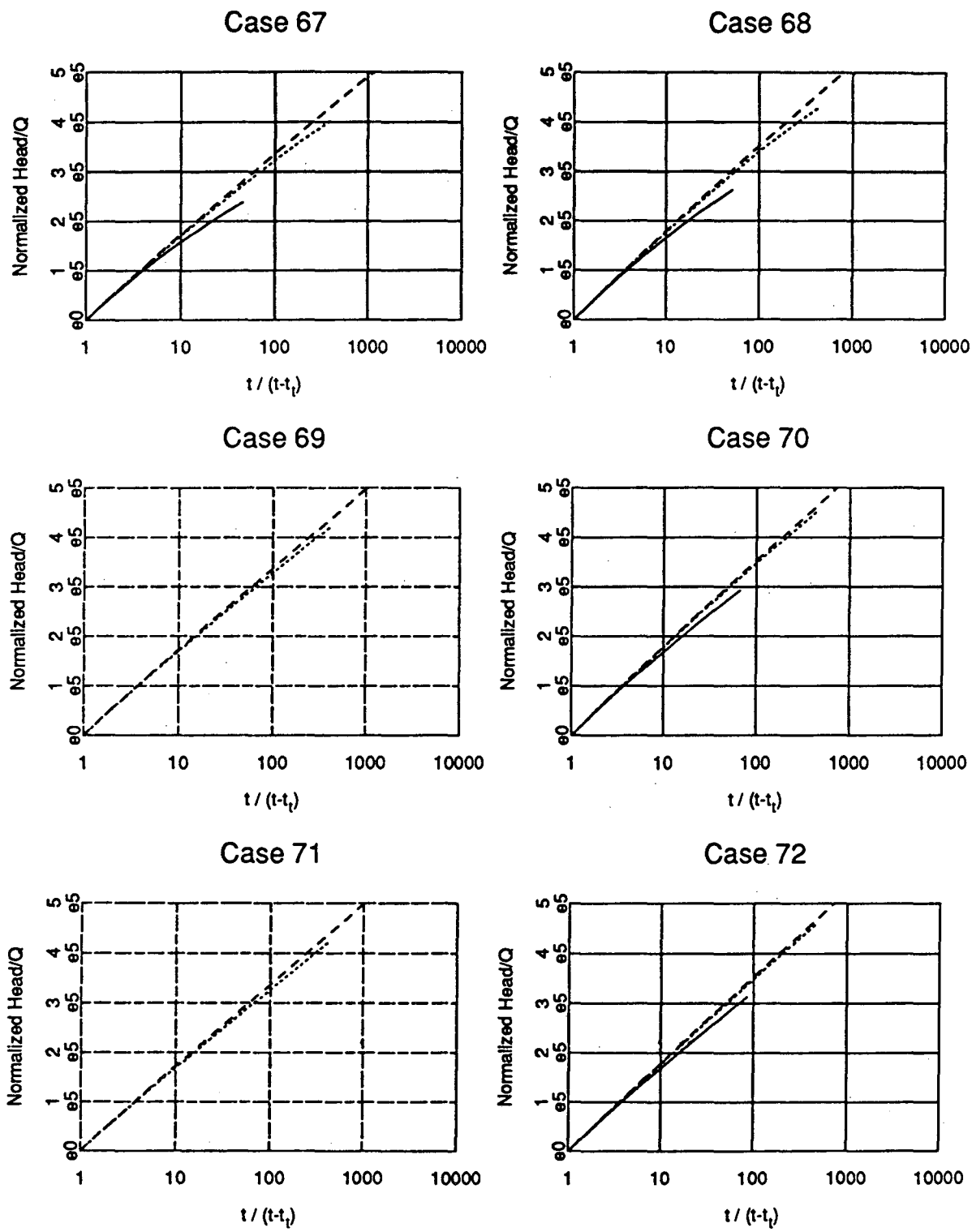

Figure A.11. Results of Case 67 through 72.

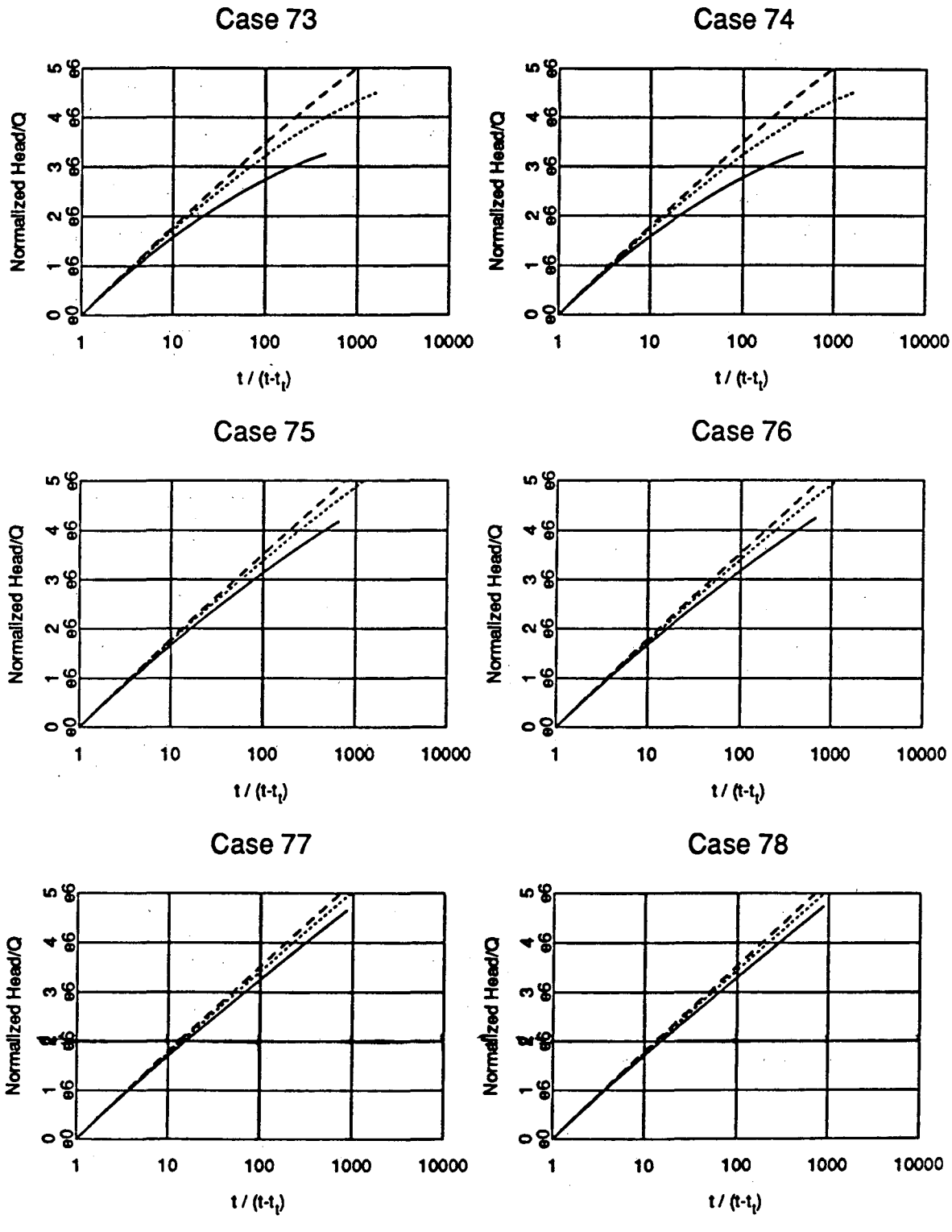

Figure A.12. Results of Case 73 through 78.

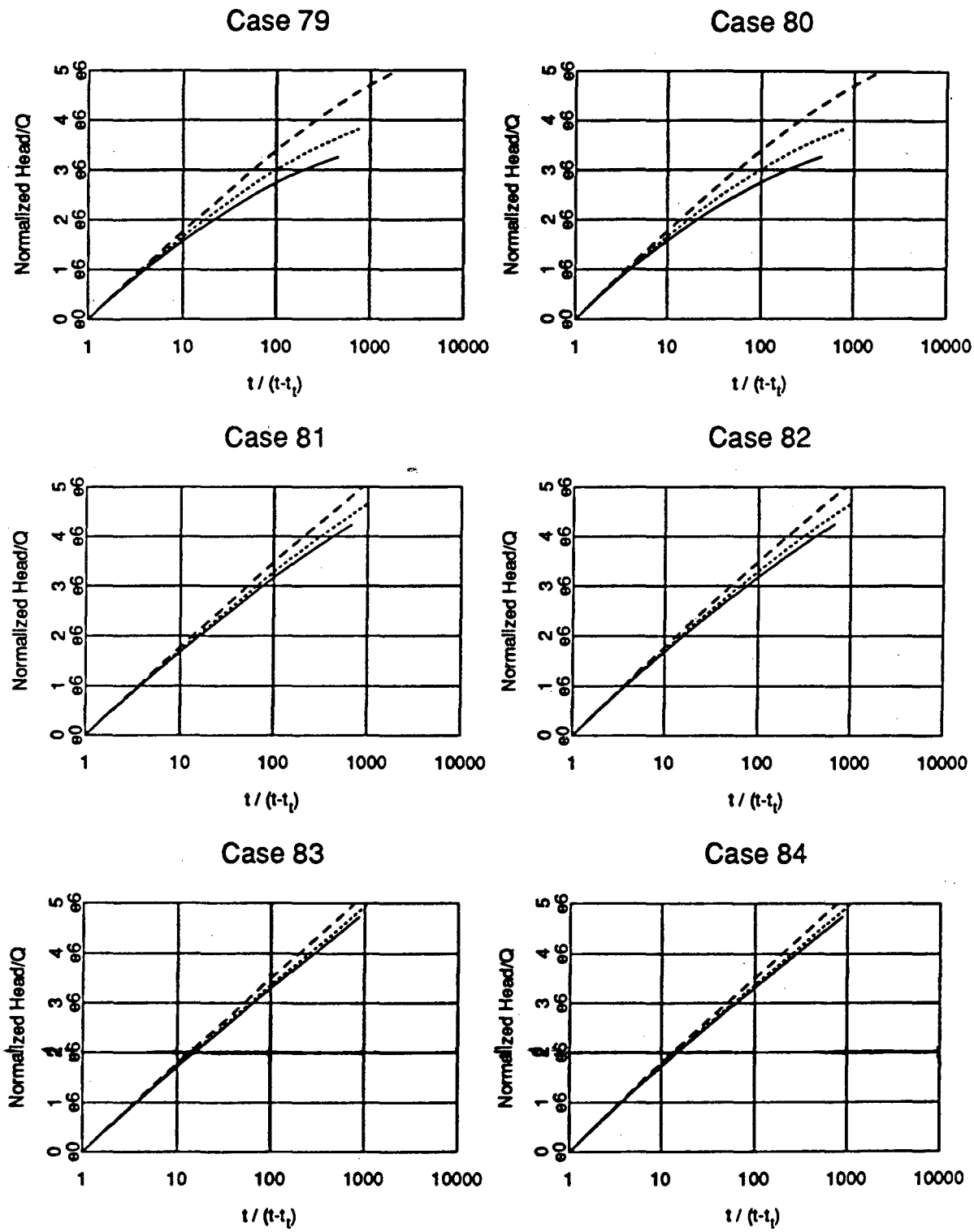

Figure A.13. Results of Case 79 through 84.

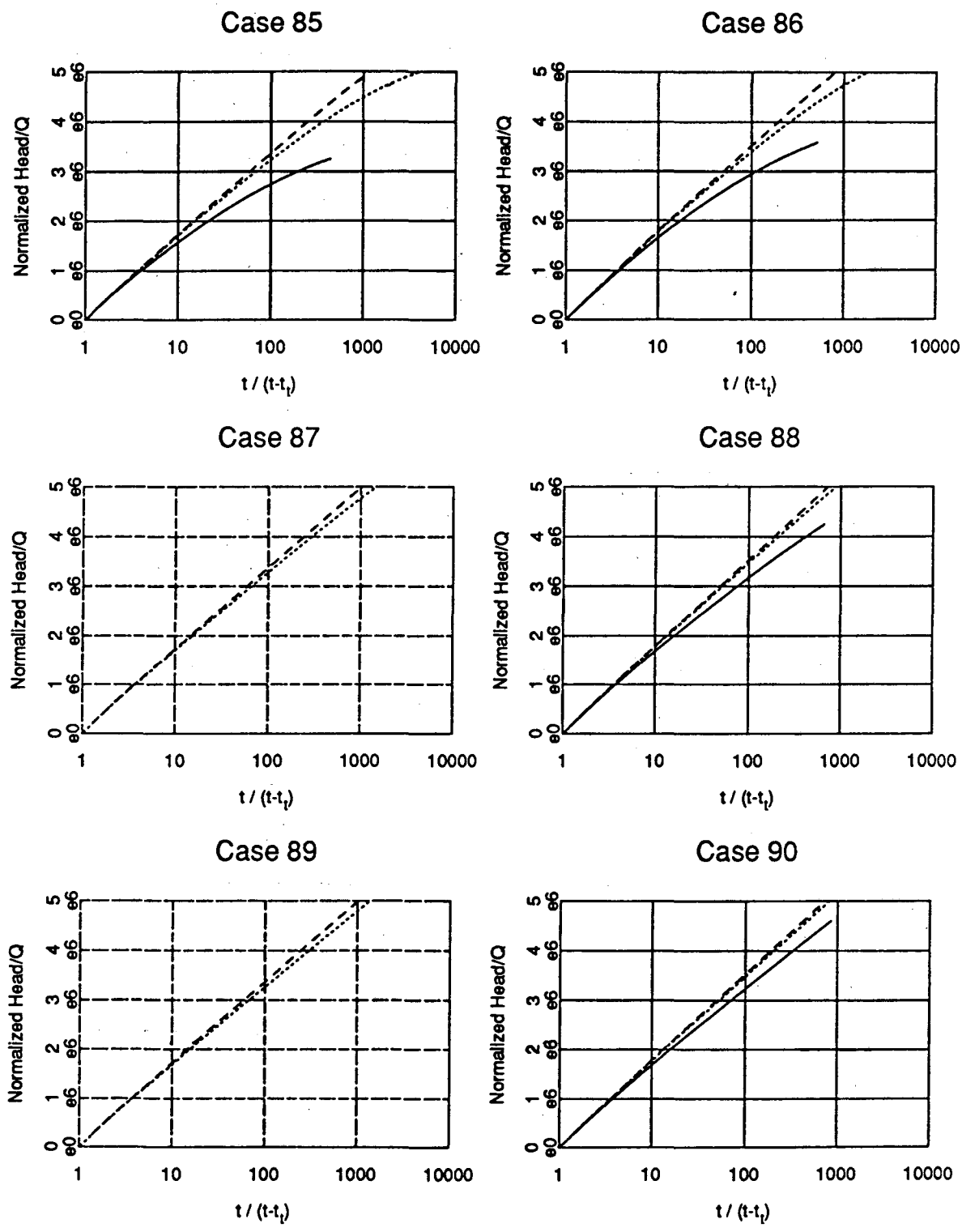

Figure A.14. Results of Case 85 through 90.

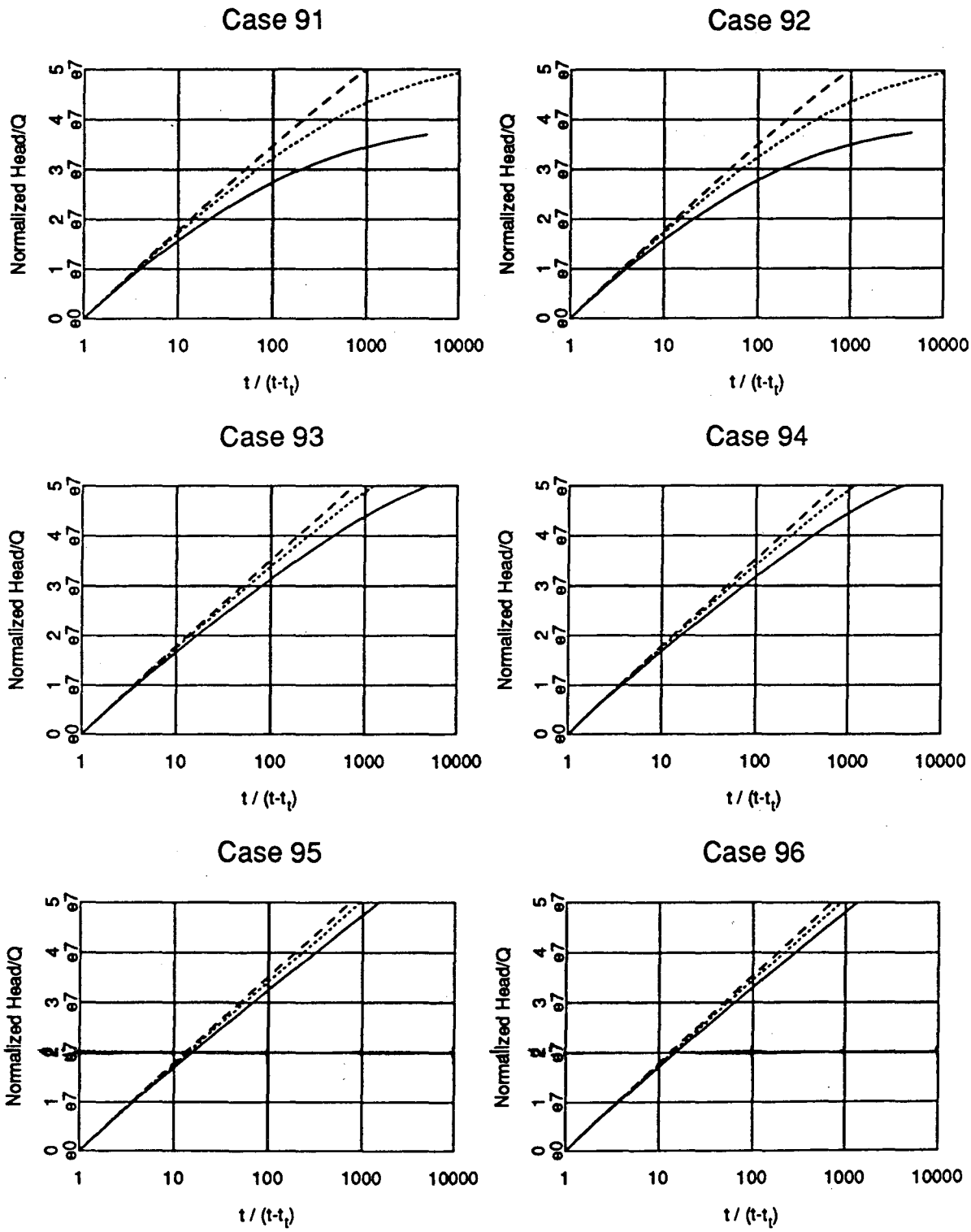

Figure A.15. Results of Case 91 through 96.

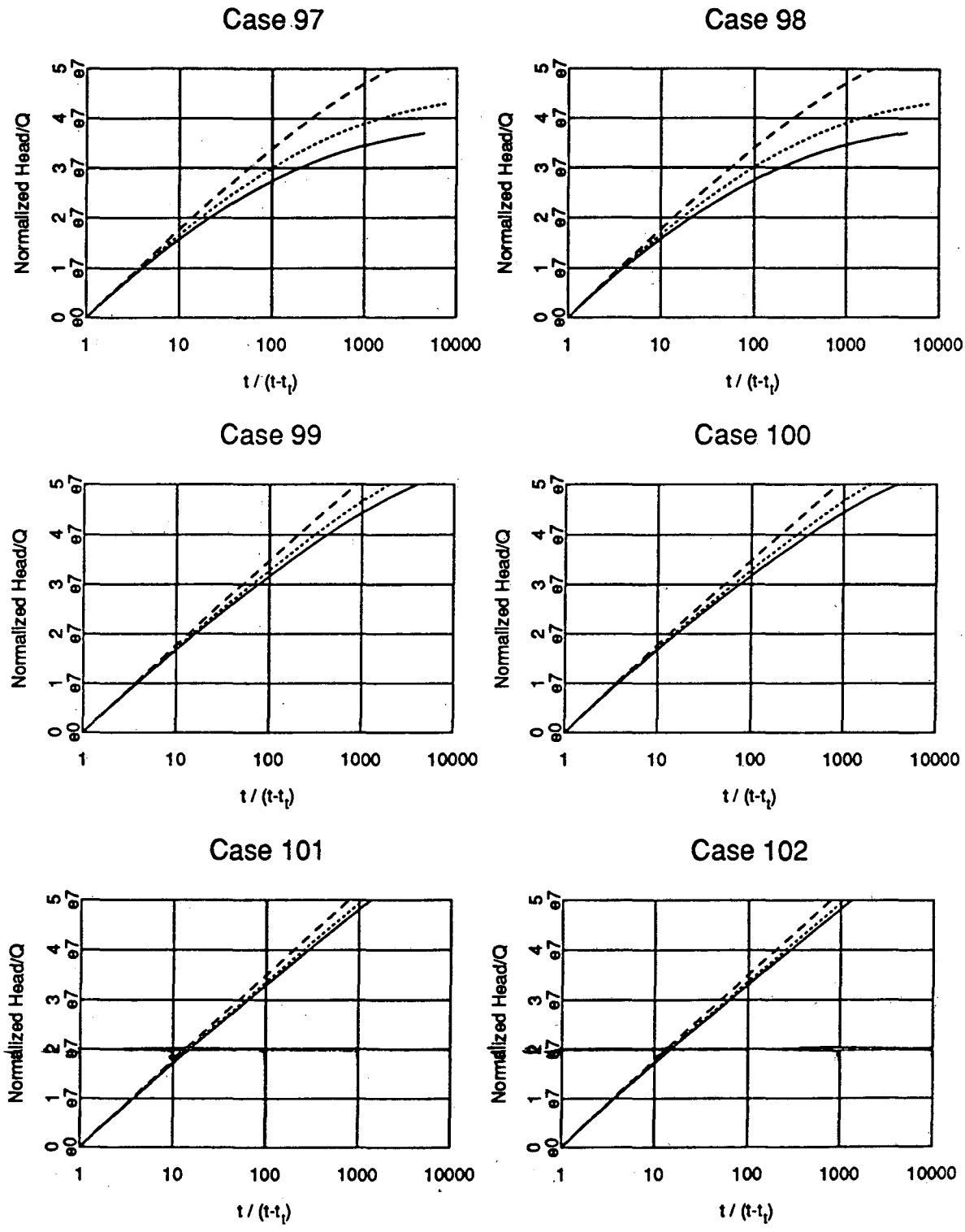

Figure A.16. Results of Case 97 through 102.

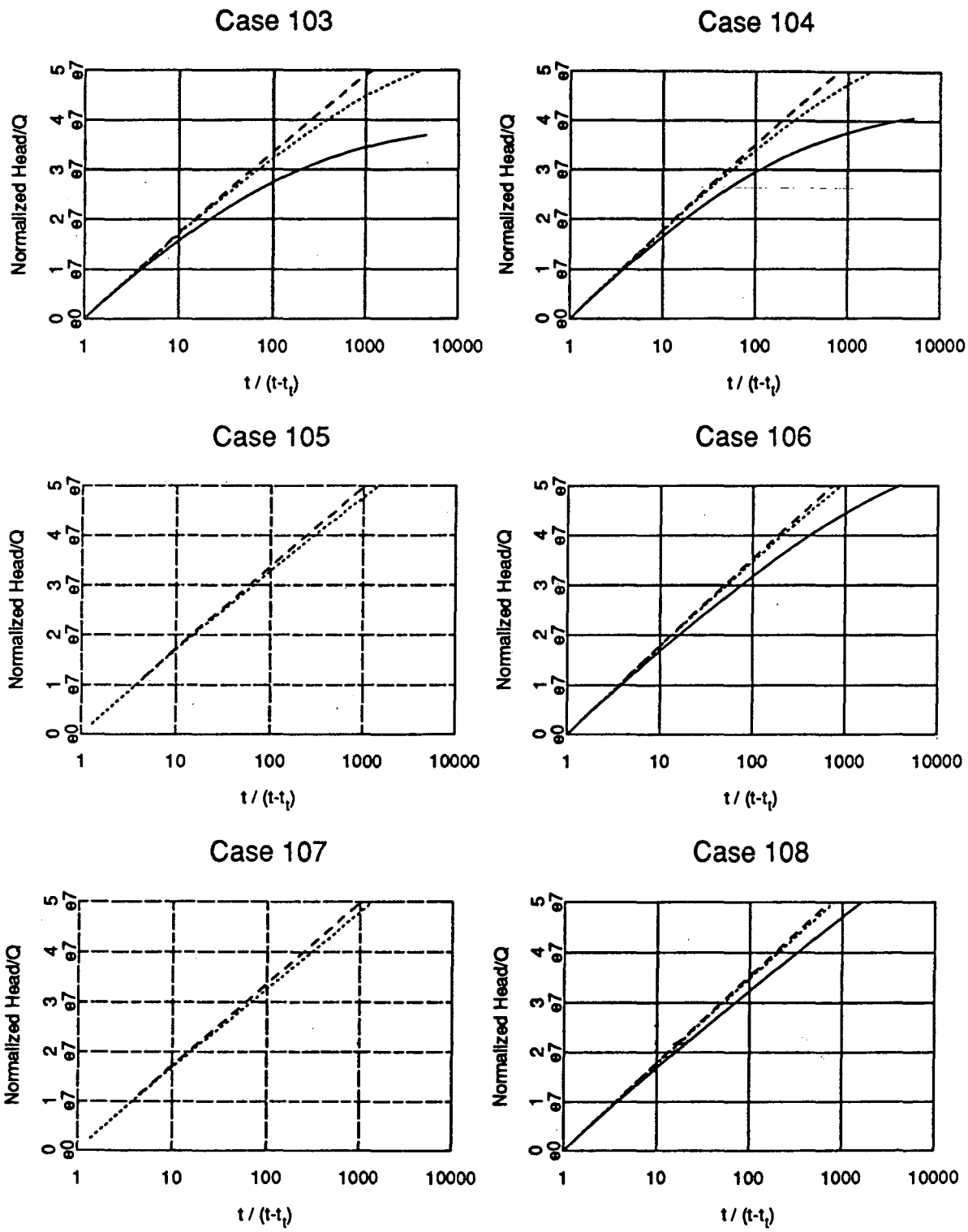

Figure A.17. Results of Case 103 through 108.

INFORMATION RESOURCES DEPARTMENT
LAWRENCE BERKELEY LABORATORY
UNIVERSITY OF CALIFORNIA
BERKELEY, CALIFORNIA 94720